

Impact of urban form on building energy consumption in different climate zones of China

Yiman Zhao ^{a,b}, Xiaotian Ding ^{a,b}, Ziyu Wu ^{a,b}, Shi Yin ^c, Yifan Fan ^{a,b,*}, Jian Ge ^{a,b}

^a College of Civil Engineering and Architecture, Zhejiang University, Hangzhou, China

^b International Research Center for Green Building and Low-Carbon City, International Campus, Zhejiang University, Haining, China

^c Institute of Energy and Power Engineering, College of Mechanical Engineering, Zhejiang University of Technology, Hangzhou 310023, China



ARTICLE INFO

Keywords:

Urban morphology
Urban heat island
Building energy consumption
Urban climate

ABSTRACT

Despite numerous studies on the relationship between urban form and building energy demand, understanding the impact mechanisms of urban form is still insufficient. Here, we identified the direct and indirect influences of urban form on building energy demand. The direct influence includes the blocking of solar radiation. The indirect influence is exerted through the urban heat island (UHI) effect as different urban forms produce different UHI intensities. The UHI effect was calculated using the urban weather generator (UWG) tool. Then, the analysis of the direct and indirect influences on the building energy demand was carried out using building energy modeling (BEM) based on the output of UWG. Five cities in different building climate zones in China were investigated, and the corresponding direct and indirect influences were quantified based on the proposed UWG + BEM framework. Results show that warmer temperatures lead to an average increase in space cooling of 16%–46% while reduced space heating of 8%–17%. The shading of surrounding buildings allows an increase of 7%–36% in space heating and a decrease of 14%–48% in space cooling compared to that of an isolated building. In addition, direct influence due to shading is prominent in Shuangyashan, Xuzhou, and Fuzhou, accounting for 50%, 80%, and 57% of variations in building energy consumption.

1. Introduction

The building sector represents a significant share of the world's energy demand [1]. Its rapid expansion in urban areas has led to a plethora of environmental issues, such as increased greenhouse gas emissions, accelerated global warming, and urban heat island (UHI) effects [2,4], altering the outdoor air temperature and wind flow [3,5,6]. Due to the interactions between indoor and outdoor environments, the energy consumption of air conditioning systems can increase [7,8]. As the urban form significantly affects the outdoor environment, its influence on building energy performance has drawn increasing attention. Numerous studies have shown that the energy consumption of buildings can be reduced by 10–30% through urban form management [9,10]. In this context, urban density and building height are important factors that affect building energy demand [11,12]. However, the impact mechanisms of urban form on building energy consumption have not been investigated, particularly in different building climate zones [23].

Urban form has two effects on building energy consumption: direct and indirect. Direct influence results from shading from surrounding

buildings, which is also referred to as the inter-building effect (IBE) [13]. IBE can reduce the heat gain from solar radiation, altering a building's energy consumption [14]. The difference in building energy performance induced by direct influence is related to the geometric information of the surrounding buildings and the intensity of solar radiation in the investigated regions. The geometry of buildings may vary across different countries due to differences in numerous factors, including government planning and construction policies, cultural customs, and topographical features [15]. Additionally, the intensity of solar radiation is affected by the region's climate [16]. A weak point of building energy models is that they typically focus on a single building [51], which is often run under isolated conditions, not accounting for adjacent buildings or simplifying them to shading geometries that are not included in the thermal balance. Many studies have shown that the influence of shading from surrounding buildings is not negligible. Pisello et al. [38] investigated the energy demands of two buildings in the isolated case and then considered the surrounding constructions. They concluded that the IBE yields strong variations by altering thermal transfers for convection and radiation. Toshiaki Ichinose et al. [14]

* Corresponding author at: College of Civil Engineering and Architecture, Zhejiang University, Hangzhou, China.

E-mail address: yifanfan@zju.edu.cn (Y. Fan).

reported that the space cooling demand decreased by as much as 10%–20%, while the space heating demand increased by up to 20%. Therefore, relevant errors may occur if the shading from surrounding buildings' contribution to energy demand is neglected.

The urban heat island phenomenon is another essential factor affected by urban form and indirectly influences building energy consumption. Sun and Augenbroe [19] studied the UHI effect in prototype office buildings in 15 climate zones in the USA and reported an average increase in cooling demand of 17.25% and a reduction in heating energy use of 17.04%. Liu et al. [20] explored the effect of UHIs on residential buildings in Singapore and reported an increase in the cooling demand of 4.15–11%. These findings indicate that the UHI effect amplifies cooling energy consumption while conversely mitigating heating energy consumption. In building thermal performance simulations that determine the energy consumption of heating, ventilation, and air conditioning (HVAC) systems, site-specific temperatures are essential inputs. Due to difficulties in obtaining onsite information, data from weather stations in rural areas or airports are usually used. However, UHI effects and microclimate variations cannot be considered under these conditions [21].

Previous methods rely on the modeling of stand-alone buildings in built environments. In recent years, there has been rapid development in chaining or coupling computational fluid dynamics (CFD) and building energy models (BEMs), i.e., the CFD-BEM framework, to consider the local climate in building energy simulations. [13,18,29,51] Given the computational cost and simulation period capabilities of CFD, it is impractical to simulate annual building energy consumption under the CFD-BEM framework. Instead, using parametric models to generate local climate data for transfer into BEMs is the most efficient way for year-long timescale simulation at the neighborhood scale. [68] In summary, a research framework chaining UWG and Design Builder, based on a deep learning-based classification of high-resolution satellite imagery, provides favorable support for evaluating the impact of building form on the annual energy consumption of buildings at the neighborhood scale. Therefore, an efficient framework is needed to evaluate both direct influence (IBE) and indirect influence (UHI).

The direct and indirect influences on building energy consumption vary across different climatic zones. Both positive and negative effects of direct and indirect influences can occur within the same city due to seasonal variations, and these differences may vary in different building climate zones. Understanding the trend of energy impact by direct and indirect influences fundamentally depends on whether the year-round climate is dominated by heating or cooling, as the heating and cooling degree days vary significantly across different building climate zones. Therefore, it is crucial to conduct quantitative research in various

background climates to understand the relationships between energy impacts and direct or indirect influences.

This study aims to investigate the mechanisms through which urban morphology affects building energy usage, considering both direct and indirect influences, to quantify the impact of these two factors on the annual energy consumption of buildings in different climate zones and explore climate-adaptive and energy-efficient building forms suitable for residential areas. By considering the key factors that affect a building's energy performance, designers and operators can make informed decisions about optimizing energy efficiency while still ensuring a comfortable and functional indoor environment.

2. Methods

Fig. 1 presents the flow chart of this study. Weather data are key information for building energy simulations for determining cooling/heating energy demands. Available weather data are usually collected in rural areas (weather stations) and cannot represent the urban heat island effect. Therefore, in this study, weather data from urban areas were collected with an urban weather generator (UWG), which simulates urban effects with the inputs of rural weather data and urban parameters. Subsequently, building energy consumption is simulated with Design Builder (Design Builder V3, Design Builder Software Ltd., UK) based on urban weather data and validated with measured building energy use data [22]. Finally, validated urban weather and energy simulation models are adopted to calculate the building energy consumption under the various layout designs, which are listed in [Section 2.4](#).

2.1. Study area

China has various climate regions with different annual average temperatures, relative humidities, precipitation amounts, etc. Based on the characteristics of local climates, China is divided into five building climate zones as shown in **Fig. 2**, including a severe cold region (Region 1), cold region (Region 2), hot summer and cold winter region (Region 3), hot summer and warm winter region (Region 4), and mild region (Region 5) [23]. Based on monthly average temperature and heating/cooling degree days as used in Ref. [14] (see **Fig. A.1** and **Fig. A.2** in Appendix A), five representative cities were chosen in five building climate zones in China, namely, Shuangyashan city (in Region 1, 46°39' N, 131°09' E), Xuzhou city (in Region 2, 34°16' N, 117°11' E), Nanjing city (in Region 3, 32°03' N, 118°48' E), Fuzhou city (in Region 4, 26°04' N, 119°18' E), and Pu'er city (in Region 5, 22°49' N, 100°54' E). The monthly average temperature accurately reflects the unique climate

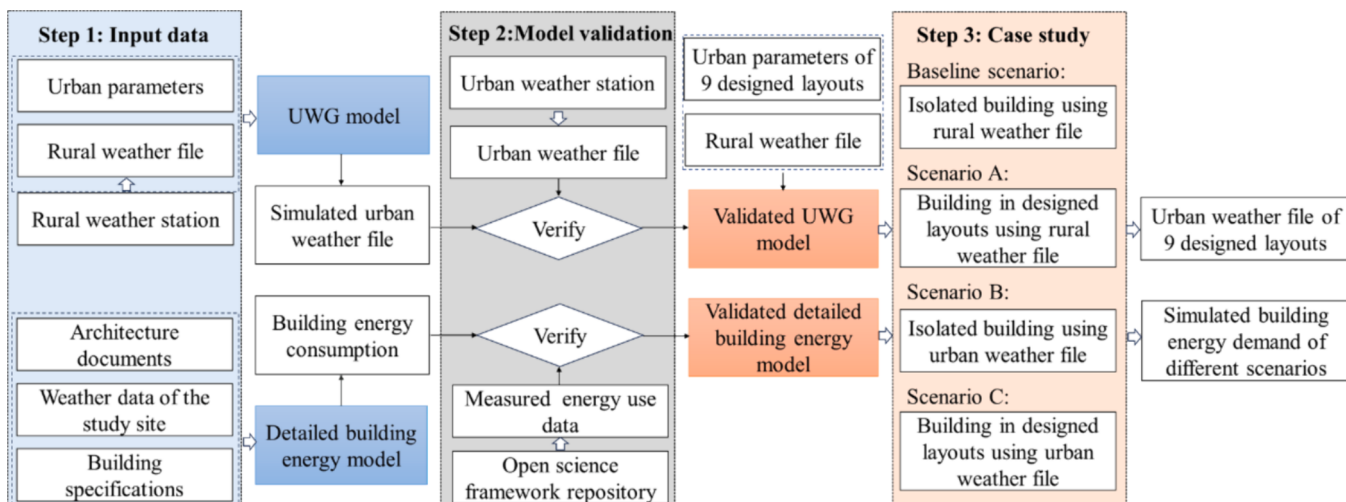


Fig. 1. Framework of this study.

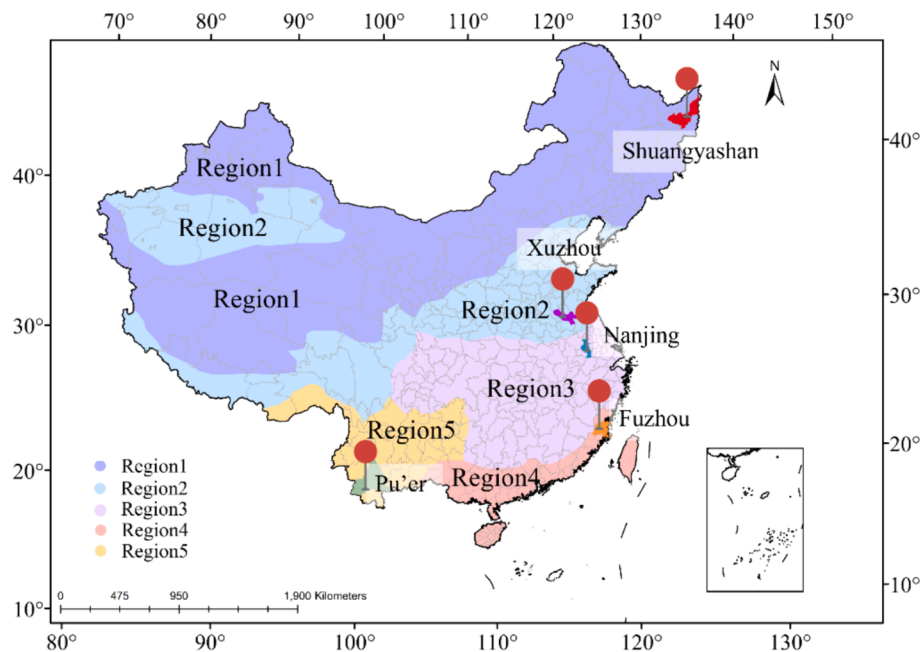


Fig. 2. Distribution of five building climate zones in China. The locations of the five cities are marked to indicate the influence of urban morphology on building energy consumption, considering both direct and indirect influences.

Table 1

Parameters of the building envelope in different building climate zones in China.

Parameters of building envelope	Region 1	Region 2	Region 3	Region 4	Region 5
Wall U value [W/m ² /K]	0.35	0.35	0.8	0.4	1.8
Roof U value [W/m ² /K]	0.2	0.3	0.4	0.7	1
Window U value [W/m ² /K]	2	2	3	6	3.5
Window-wall ratio	0.25				
Window SHGC	0.45	0.45	0.30	0.15	0.30
Infiltration rate (ACH)	0.5	0.5	1	1	0.5
Lighting load density [W/m ²]	5				
Equipment load density [W/m ²]	3.8				
Occupancy density [m ² /person]	25				
Heating/Cooling temperature [°C]	20/26				

characteristics of each city within its respective climate zone. Furthermore, information on heating and cooling degree days offers valuable insights into energy consumption patterns, consolidating cities' representativeness within their respective building climate zones.

In this study, a typical residential building model was created to simulate energy demand in five major building climate zones (region 1 to region 5). The typical residential building layout and geometric parameters (Fig. A.3 in Appendix A) were determined through cluster analysis of existing Chinese residential buildings [30]. The typical building comprised two flats on each floor. The total area of an apartment is 113 m². According to the statistics on housing area per capita published by the National Bureau of Statistics [31], we assume three people (one household) in one suite. The building envelope performance-related parameters (Table 1) were set according to the building design standards [66,67,69,70].

2.2. Validation of the UWG model

As an alternative to computationally expensive numerical models, Bueno et al. [24] proposed an urban weather generator (UWG) to estimate the UHI effect in the urban canopy layer using rural weather data measured at an operational weather station outside the city, and urban parameters including the average building density, average building height, the facade to site ratio, as well as the fraction of tree/grass cover. In this study, Fuzhou city was selected to validate the UWG model due to

the availability of a pair of weather stations serving both rural and urban areas. Fuzhou has a typical subtropical humid monsoon climate with an average temperature of 20.7 °C in 2019.

The rural weather data were collected from the weather station in Luoyuan County (26°30' N, 119°33' E), which is located in an open rural area approximately 50 km from the urban weather station (31°36' N, 119°04' E) of Fuzhou city. The region is surrounded by farmland, and the station undergoes regular maintenance to ensure the quality and consistency of the data. The urban weather station is located in a built-up area of Fuzhou city. The locations and surroundings of urban and rural weather stations in Fuzhou city are shown in Fig. B.1. Urban morphological data with a 500 m buffer zone around the Fuzhou weather station were extracted using ArcGIS 10.2 (ArcGIS 10.2, Esri, United States). Moreover, as shown in Fig. 3, the deep learning-based high-resolution satellite imagery classification method [50] has been employed to extract urban vegetation cover information, including tree cover and grass cover. In this method, a land cover dataset (satellite imagery and corresponding land cover map) was first built with a semimanual approach [50]. The dataset, along with additional satellite images from Google Earth, was used to train and validate a deep learning image classification model [51], which can be applied to classify satellite images into seven land cover categories, including "grass", "tree", "road", "shadow", "water", "building" and "impervious (other impervious surface)". In this study, we used the fractions of "building", "grass" and "tree" in the resulting land cover map as input parameters

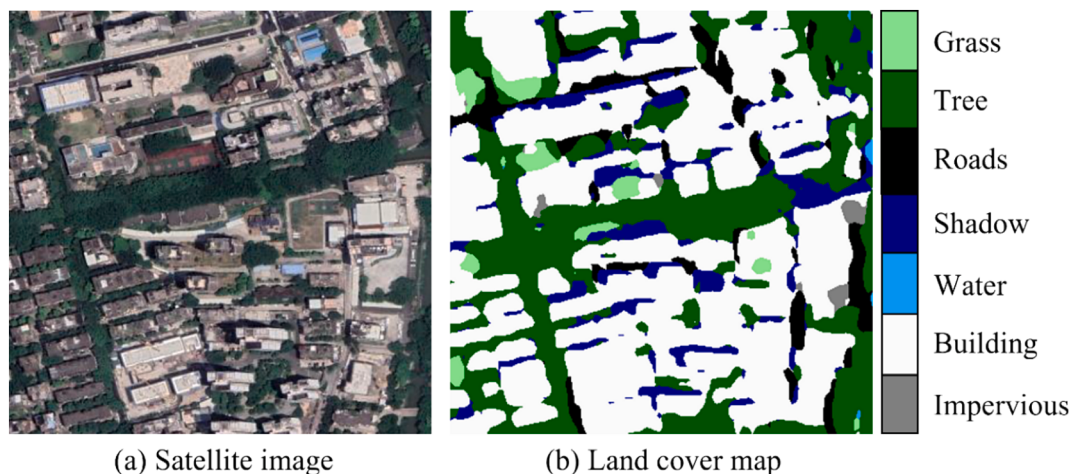


Fig. 3. Results of land cover classification. (a) Satellite image of a 500 m buffer zone around an urban weather station in Fuzhou city. (b) Land cover classification result after transfer learning.

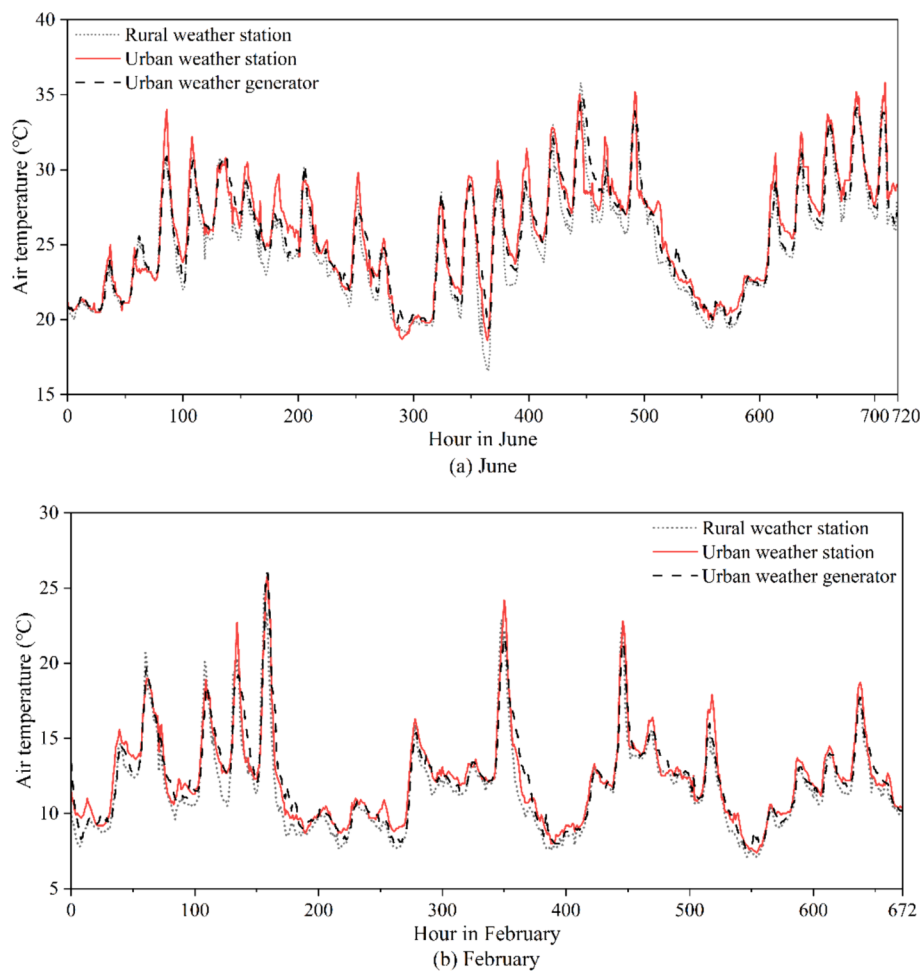


Fig. 4. Comparison of hourly temperatures at Fuzhou weather stations with simulated hourly temperatures at the city weather generator. (a) June (summer month). (b) February (winter month).

for UWG. Urban parameters (see Table B.1 in Appendix B) were obtained and combined with rural weather data to simulate urban weather data using UWG.

Hourly urban weather data were collected from the China Meteorological Data Network (<http://data.cma.cn/>, accessed in December 2019). The simulated hourly temperature data are compared with urban

weather station data to validate the accuracy of the UWG, as shown in Fig. 4. As shown in Fig. 4, the temporal variation in urban temperature can be captured well by the UWG model in this study. The annual root mean square error (RMSE) is 1.37 K. To be clear and concise, only the data from June and February are presented here. The RMSE was 1.09 K in June and 1.13 K in February. The UWG model has been widely used in

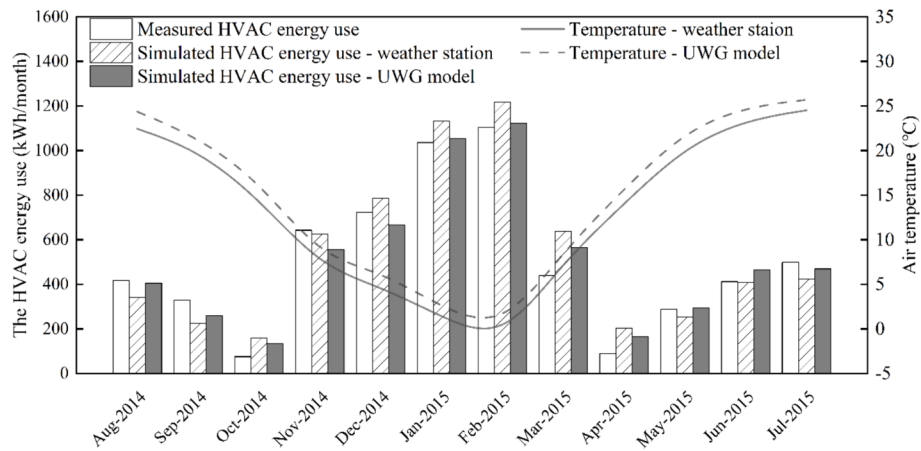


Fig. 5. Monthly HVAC energy consumption (kWh/month) from measurements and simulations and the measured and simulated monthly average air temperature.

previous studies in different cities, such as Toulouse (France), Basel (Switzerland) [24], Boston [25], Vienna [26], Rome, and Barcelona [27], where the RMSE for the above applications ranges from 1.0 to 2.6 K [27]. This indicates that the UWG model in this study can be used in different design layouts to account for UHIs.

2.3. Validation of the building energy simulation model

A dataset provided by the Open Science Framework repository [28] was used to validate the building energy simulation model. The dataset includes measured energy use data and architectural and engineering documents of a building explicitly designed and operated as a zero-energy building located in Charlottesville, Virginia, USA ($38^{\circ}01'12''N$, $78^{\circ}29'24''W$). The building model is shown in Fig. B.2. Weather data were collected from the Charlottesville Meteorological Station (Charlottesville, VA Weather History | Weather Underground) between August 2014 and July 2015, which can be used as inputs to simulate building energy in accordance with the building specifications outlined in Ref. [22].

The above rural weather data and urban parameters (see Table B.2 in Appendix B) were also input into the UWG model to generate urban

weather data. The measured energy use data, simulations based on rural weather data and simulations based on urban weather data were then compared and are shown in Fig. 5. The RMSEs for the annual HVAC energy consumption using the rural and urban weather data (simulated by UWG based on the rural weather data) are 95.66 kWh and 61.37 kWh, respectively, which is an improvement of 36 %. Based on previous literature [29], the simulation model error (1.7 %) in the present study falls within an acceptable range.

2.4. Case study description

Based on the typical residential building layouts in China [30], nine layouts are designed, as shown in Fig. 6, including open low-rise buildings (Layout 1), medium-density low-rise buildings (Layout 2), compact low-rise buildings (Layout 3), open mid-rise buildings (Layout 4), medium-density mid-rise buildings (Layout 5), compact mid-rise buildings (Layout 6), open high-rise buildings (Layout 7), medium-density high-rise buildings (Layout 8) and compact high-rise buildings (Layout 9). The average building height and area density of the nine layouts are shown in Table 2. The values of the building height and density are set based on national standards. [35,67].

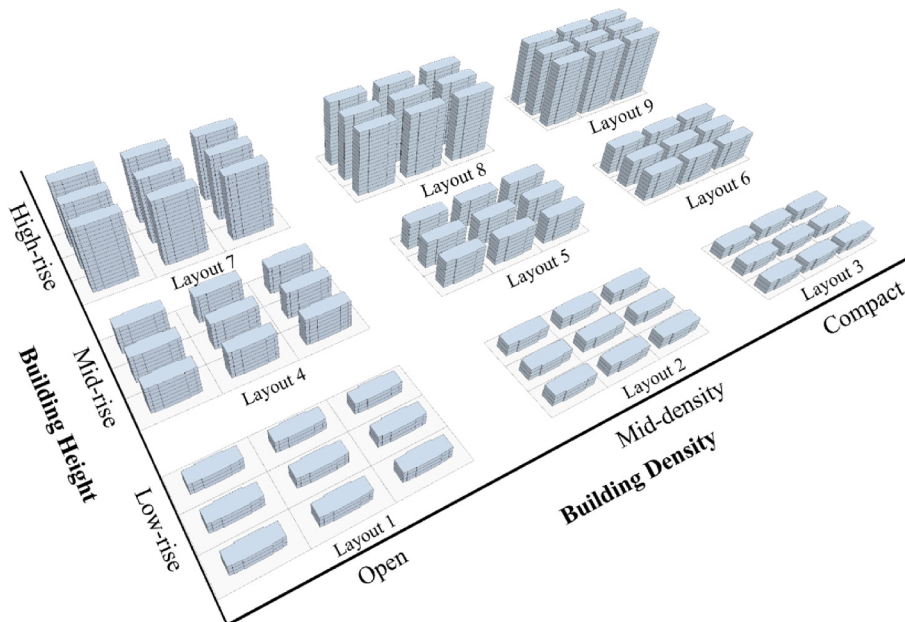


Fig. 6. Configuration of urban areas in 9 designed layouts.

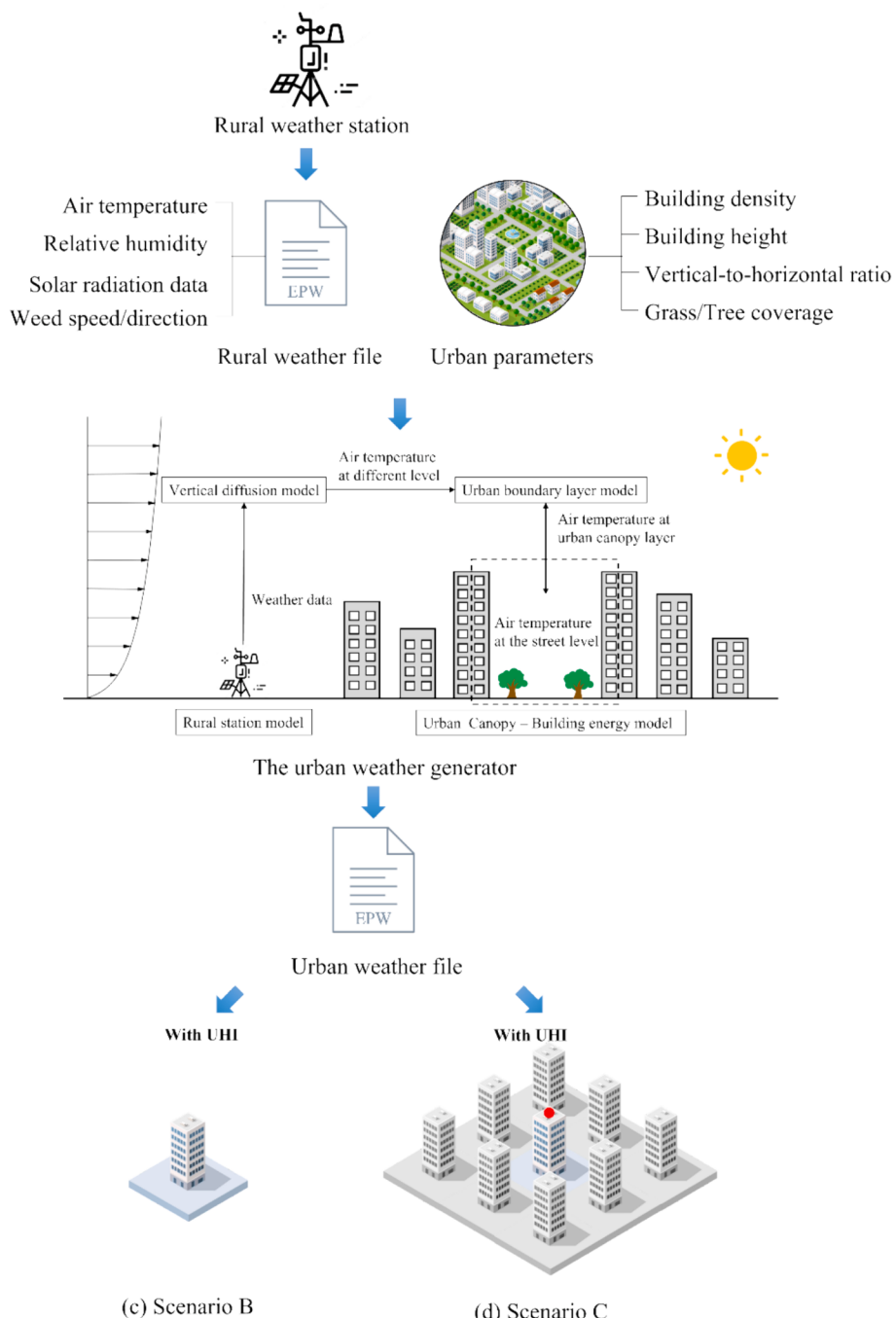
Table 2

Description of urban areas in 9 designed layouts.

Description	Average building height	Building density	
Layout 1	Open Low-Rise	9 m	0.25
Layout 2	Mid-density Low-Rise	9 m	0.35
Layout 3	Compact Low-Rise	9 m	0.45
Layout 4	Open Mid-Rise	21 m	0.25
Layout 5	Mid-density Mid-Rise	21 m	0.35
Layout 6	Compact Mid-Rise	21 m	0.45
Layout 7	Open High-Rise	45 m	0.25
Layout 8	Mid-density High-Rise	45 m	0.35
Layout 9	Compact High-Rise	45 m	0.45

To quantify the direct and indirect influences, we employed a baseline scenario and three other scenarios based on different layout conditions to simulate the target building's cooling and heating energy demands, as shown in Fig. 7. A total of 150 cases were included, including 135 cases [5 (Regions) \times 3 (Scenarios) \times 9 (Layouts) = 135] for the target buildings within the urban block and 15 base cases [5 (Regions) \times 3 (Building Heights) = 15] for the isolated building layout.

In the nine-dimensional layout, the target building is located at the centre of a group of buildings to consider direct influence, i.e., blocking solar and longwave radiation. As a baseline scenario shown in Fig. 7a, an isolated building located in a rural area is adopted, which will not account for direct influence or indirect influence. Fig. 7b shows Scenario A, which focuses on the simulation process and considers only direct influence. The target building is positioned in the middle of the

**Fig. 7.** Schematic diagram of the simulation process. (a) Baseline scenario; (b) Scenario A; (c) Scenario B; (d) Scenario C.

building group, accounting for direct influence. The input meteorological data were obtained from rural weather stations. Therefore, indirect influence is not considered in Scenario A. In Fig. 7c, Scenario B illustrates the simulation process that solely considers indirect-influence. The isolated buildings are located in urban areas without any surrounding obstructions. Consequently, when simulating the energy consumption of target buildings, meteorological data are generated using the UWG to simulate the urban climate based on the characteristics of the urban morphology and rural weather stations. Fig. 7d shows Scenario C, which incorporates both direct and indirect influences.

To quantify the impact of urban form on building energy consumption, we use the relative change rate [17] (R) defined as the relative

increase (decrease) in the cooling and heating energy demands of the target building modelled under different layouts, as in Eq. (1).

$$R = \frac{E_i - E_{\text{baseline scenario}}}{E_{\text{baseline scenario}}} \quad (1)$$

where i represents different layouts, where $i = 1, 2, 3\dots, 9$. E denotes the cooling and heating energy demands of the target building. The values of R reflect how the cooling/heating energy demands of target buildings are impacted by urban form. $R \geq 80$ indicates a rise in energy demand for the target building due to the urban form, whereas $R < 80$ means that the target building in the urban grid is more energy efficient than an isolated building.

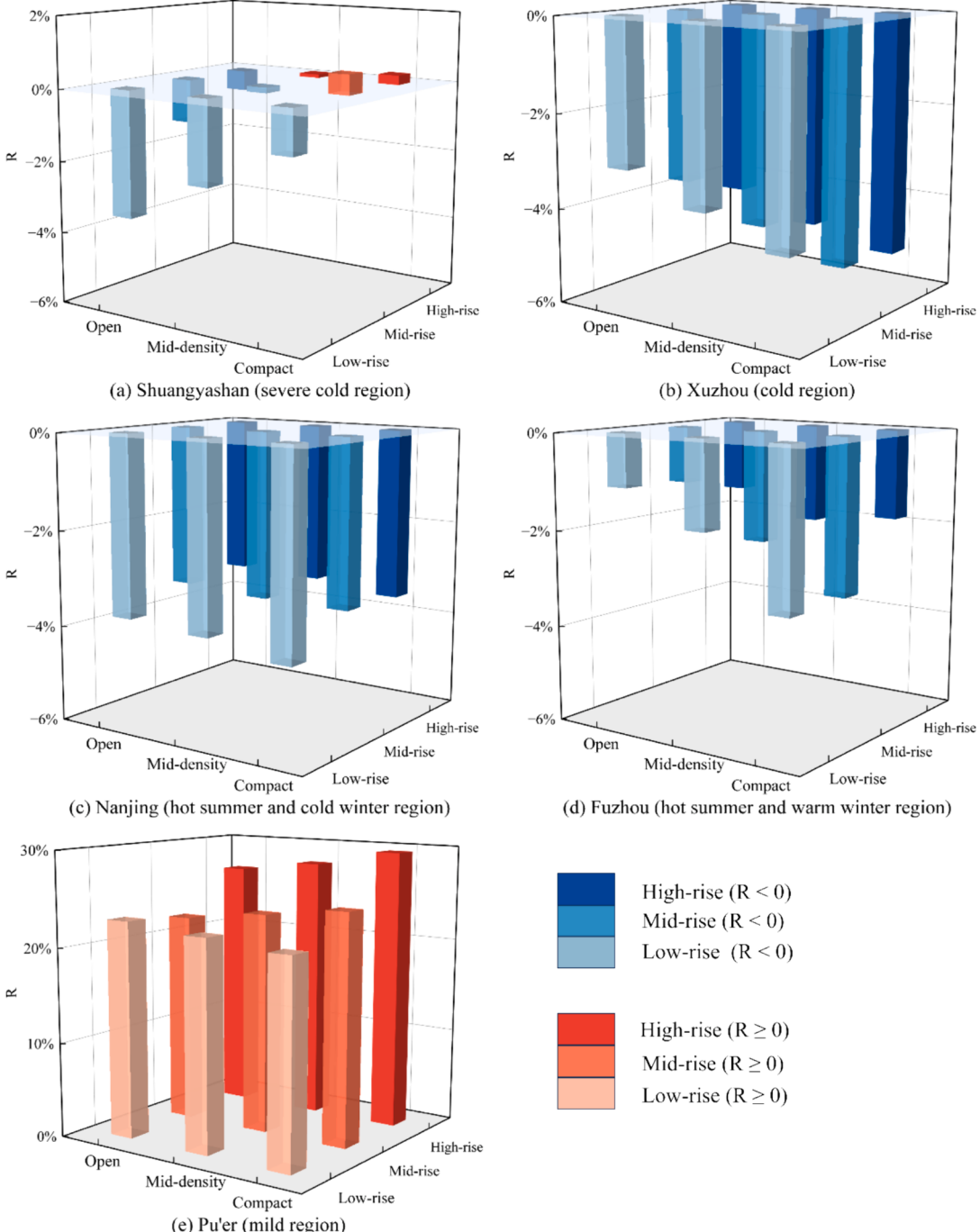


Fig. 8. The relative change in R for annual energy consumption in cities represents five climate zones in China. (The color blue is used to represent $R < 80$, while the color red is used to represent $R \geq 80$.) (For interpretation of the references to color in this figure legend, the reader is referred to the web version of this article.)

To further evaluate the relative significance of direct and indirect influences, we defined two ratios, RID (Eq. (2)) and RII (Eq. (3)), which represent the relative importance of direct and indirect influences, respectively.

$$\text{RID} = \frac{\Delta E_D}{\Delta E_D + \Delta E_I} \quad (2)$$

$$\text{RII} = \frac{\Delta E_I}{\Delta E_D + \Delta E_I} \quad (3)$$

where ΔE_D (defined in Eq. (4)) represents the absolute value of the change in cooling/heating energy demands due to direct influence. ΔE_I (defined in Eq. (5)) represents the absolute value of the change in cooling/heating energy demands due to indirect influence.

$$\Delta E_D = |E_i, \text{ scenario A} - E_i, \text{ baseline scenario}| \quad (4)$$

$$\Delta E_I = |E_i, \text{ scenario B} - E_i, \text{ baseline scenario}| \quad (5)$$

where i represents different layouts, where $i = 1, 2, 3 \dots, 9$. E denotes the cooling and heating energy demands of the target building. Specifically, RID and RII indicate the proportion of direct or indirect influence that contributes to the overall influence, respectively. A ratio greater than 50 % indicates that direct influence makes a relatively larger contribution and vice versa.

For the nine layouts of urban form, the time series of urban and rural temperatures denoted as $T_{URB}(t)$ and $T_{RUR}(t)$, respectively, were obtained. $T_{RUR}(t)$ is from measurements of rural weather stations in the corresponding cities. $T_{URB}(t)$ is calculated with the UWG based on the $T_{RUR}(t)$ and the building layouts in appropriate cases. Therefore, the urban heat island intensity (UHII) at a specific time t can be expressed as

Table 3

The actual heating and cooling demand and the rate of change in relation to isolated buildings in the five representative cities.

City name	Heating demand (kW/m^2)			Cooling demand (kW/m^2)			Annual R (%)
	$E_{\text{baseline scenario}}$	$E_{\text{Scenario C}}$	$R_{\text{heating}} (\%)$	$E_{\text{baseline scenario}}$	$E_{\text{Scenario C}}$	$R_{\text{cooling}} (\%)$	
Shuangyashan	124.2	124.4	0.1	5.4	4.3	-19.2	-0.7
Xuzhou	43.5	41.9	-3.8	30.6	29.7	-2.9	-3.5
Nanjing	79.3	71.1	-10.3	37.0	41.0	10.8	-3.6
Fuzhou	28.4	25.3	-11.1	63.2	64.5	2.0	-2.0
Pu'er	13.8	14.8	7.1	55.4	71.3	28.9	24.4

Note: Negative R values indicate that space cooling or heating demand will be reduced; otherwise, positive R values indicate an increase. In other words, if the direct and indirect influences are considered, the demand for space cooling or heating will increase or decrease.

Table 4

The relative importance of the direct influence (RID) and indirect influence (RII) of nine urban forms throughout the year.

	Shuangya-shan		Xuzhou		Nanjing		Fuzhou		Pu'er	
	RII (%)	RID (%)	RII (%)	RID (%)	RII (%)	RID (%)	RII (%)	RID (%)	RII (%)	RID (%)
	Layout 1	68	32	21	79	62	38	43	57	91
Layout 2	57	43	21	79	62	38	41	59	88	12
Layout 3	49	51	19	81	63	37	37	63	86	14
Layout 4	52	48	28	72	83	17	45	55	83	17
Layout 5	47	53	24	76	85	15	42	58	82	18
Layout 6	43	57	19	81	79	21	41	59	82	18
Layout 7	48	52	24	76	88	12	46	54	85	15
Layout 8	45	55	15	85	90	10	45	55	84	16
Layout 9	44	56	10	90	55	45	46	54	84	16
Average	50	50	20	80	74	26	43	57	85	15

Note: Green indicates relatively greater relative importance in directly or indirectly affecting the demand for year-round cooling and heating.

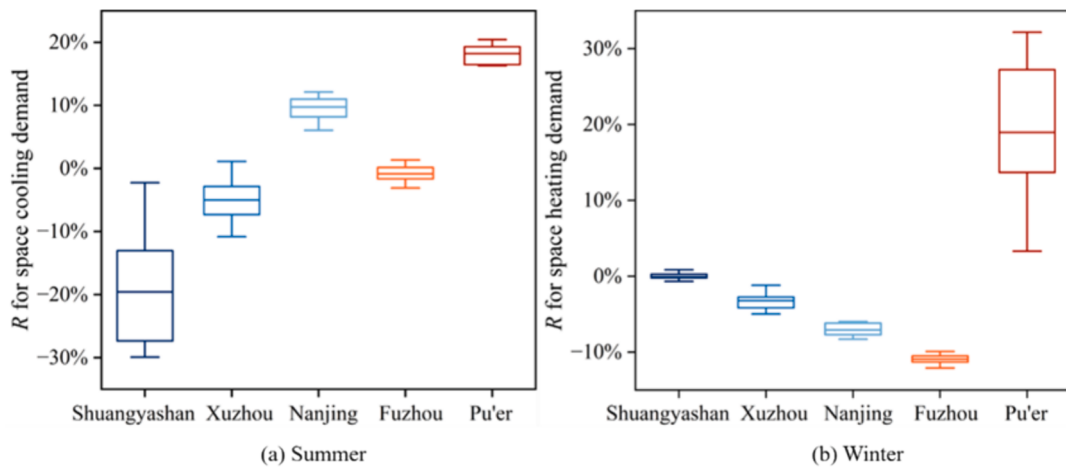


Fig. 9. R for (a) the space cooling demand and (b) the heating demand of the target building in different cities. (The upper and lower limits in a box plot typically represent the maximum and minimum values in the data set, while the box itself represents the interquartile range of the data. The horizontal line inside the box represents the median value.).

Table 5

The relative importance of direct influence (RID) and indirect influence (RII) for nine urban form cases in summer.

Layout	Shuangyashan-han		Xuzhou		Nanjing		Fuzhou		Pu'er	
	RII (%)	RID (%)	RII (%)	RID (%)	RII (%)	RID (%)	RII (%)	RID (%)	RII (%)	RID (%)
Layout 1	51	49	51	49	71	29	54	46	89	11
Layout 2	44	56	43	57	64	36	49	51	82	18
Layout 3	39	61	37	63	57	43	43	57	75	25
Layout 4	44	56	42	58	63	37	49	51	70	30
Layout 5	40	60	38	62	58	42	45	55	66	34
Layout 6	39	61	35	65	56	44	43	57	64	36
Layout 7	41	59	39	61	62	38	48	52	69	31
Layout 8	39	61	37	63	59	41	46	54	65	35
Layout 9	40	60	36	64	58	42	46	54	64	36
Average	42	58	40	60	61	39	47	53	72	28

Note: The values filled with blue indicate a relatively greater relative importance in directly or indirectly affecting the demand for cooling in summer.

and, conversely, a positive effect in layouts 1–9. The direct influence is more pronounced for taller or denser buildings, which results in increased energy consumption. This suggests that lower building density and heights are conducive to reducing building demands in Shuangyashan city. This suggests that lower building density and heights are conducive to reducing building demands in Shuangyashan city. Similarly, the previous study [52,53] used regression analysis of the residential morphology factor and heating energy consumption in Harbin, a severely cold region, and the results showed that building density was positively correlated with the intensity of residential heating energy consumption. Table 4 provides a breakdown of the impacts, showing that indirect influence accounts for 58 % and 56 % of the overall impacts of the low-rise building layout (average of layouts 1–3) and open building layout (average of layouts 1, 4 and 7), respectively. The study also revealed that 68 % of the overall impact on energy consumption is attributable to the indirect influence of the Layout 1 condition.

Fig. 8b and 8c illustrate the influences of urban form in Xuzhou and Nanjing city, respectively. In Xuzhou (Region 2), high-rise and high-density building layouts exhibit lower annual heating and cooling energy consumption than isolated building layouts, with 4.7 % and 4.9 %

reductions, respectively. Furthermore, compact high-rise building layouts can reduce cooling and heating energy demands by up to 5.2 %. The heating and cooling demand of the target buildings in all nine urban forms in Xuzhou was lower than that of the isolated buildings in rural areas, with an average annual demand 3.5 % lower (see Table 3). The annual heating/cooling energy demands decrease as the density and height increase. A significant proportion of the overall impact on energy consumption (an average of 80 %) is attributed to direct-influences on the various urban forms. The reduction in the cooling demand due to direct influence is more significant than the increase in the heating energy demand [54].

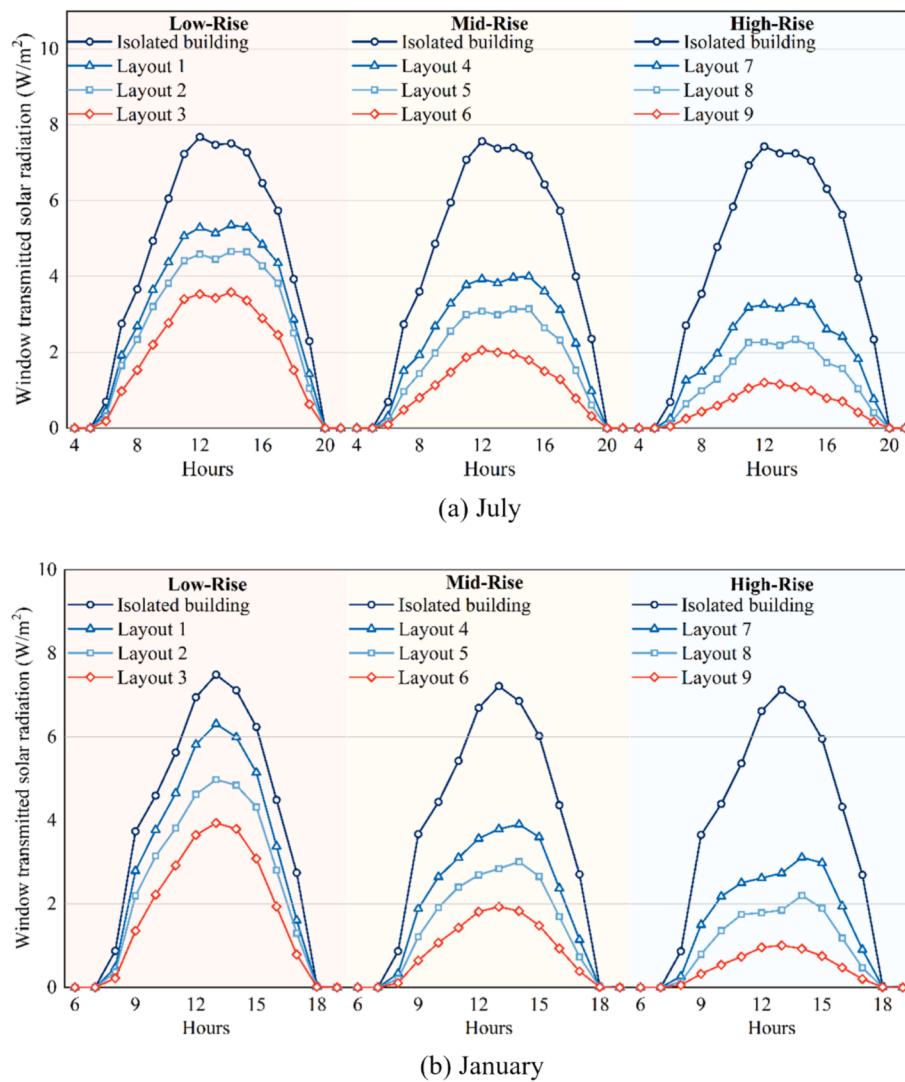
For Nanjing city (Region 3), the average annual relative rate of change in cooling/heating energy demand is −3.6 %, which does not significantly differ among urban forms. The results for cooling and heating demand for the target buildings in the nine urban forms show an average decrease in heating demand of 10.3 % and an average increase in cooling demand of 10.8 % compared to isolated buildings (see Table 3). This indicates the predominance of indirect influences. Moreover, Table C.2 shows that the IBE leads to a reduction in annual cooling and heating energy consumption of 1.1 % (0.2 %–4.8 %). This

Table 6

The relative importance of direct influence (RID) and indirect influence (RII) for nine urban form cases in winter.

Layout	Shuangya-shan		Xuzhou		Nanjing		Fuzhou		Pu'er	
	RII (%)	RID (%)	RII (%)	RID (%)	RII (%)	RID (%)	RII (%)	RID (%)	RII (%)	RID (%)
Layout 1	62	38	74	26	85	15	89	11	13	87
Layout 2	53	47	64	36	76	24	82	18	11	89
Layout 3	49	51	56	44	68	32	73	27	16	84
Layout 4	50	50	60	40	70	30	72	28	38	62
Layout 5	47	53	55	45	65	35	66	34	31	69
Layout 6	46	54	53	47	63	37	62	38	27	73
Layout 7	49	51	57	43	68	32	64	36	30	70
Layout 8	48	52	54	46	65	35	66	34	27	73
Layout 9	49	51	54	46	74	26	62	38	25	75
Average	50	50	59	41	71	29	71	29	24	76

Note: Red indicates relatively greater relative importance in directly or indirectly affecting the demand for heating in winter.

**Fig. 10.** Daily trends in average solar heat gain through windows in Xuzhou city. (a) July, (b) January.

finding aligns with a study in Nanjing [14], which revealed that annual cooling and heating demand is reduced by 2.69 % to 12.60 % due to the shading effect of the surrounding buildings. In addition, indirect influence dominates, accounting for an average of 74 % of the overall impact on energy consumption.

For Fuzhou city (Region 4, hot summer and warm winter region), the cooling demand dominates. The annual cooling demand of the nine urban forms is 2.0 % lower on average than that of the isolated building layout in the baseline scenario. According to Table 3, the heating demand shows an average decrease of 11.1 %, while the cooling demand shows an average increase of 2.0 %, which indicates that UHIs play a dominant role throughout the year. However, direct or indirect influences can cancel each other out during the year, e.g., direct influences result in lower cooling energy consumption in summer and higher heating energy consumption in winter. Table C.1 shows indirect influences have a significant but almost total offsetting effect on cooling and heating demand. Direct influences have a more pronounced positive effect on cooling energy consumption, i.e., lower annual cooling and heating demand, than for isolated buildings.

Therefore, direct influence accounts for 57 % of the overall impact on energy demand, while the remaining 43 % is attributed to indirect influence from an annual perspective. For each urban form, the direct influence on energy consumption has a more significant influence. These results indicate that IBE plays a dominant role in the impact of annual energy consumption on the nine building forms in Fuzhou city, resulting in a decrease in the yearly cooling demand. The effects of shading on space cooling and heating demand in Fuzhou are the same as those in Ichinose [14]. Additionally, the effect of shading on the space cooling energy demand is more pronounced than that on the heating energy demand based on the results showing that the percentage is more significant in summer. In addition, the availability of overshadowing from adjacent buildings in high-density neighborhoods has been found to reduce heat gain from direct irradiation in climates where the cooling demand is dominant [62,63].

As shown in Fig. 8e, the cooling and heating energy demands of the target buildings are 20–30 % greater than those of isolated building layouts in various urban forms annually in Pu'er (region 5). Table 3 shows an average increase of 24.4 % relative to isolated building layouts in cooling and heating energy demands in Pu'er. Specifically, the cooling demand experiences an average increase of 28.9 %. Indirect influence was responsible for an average of 85 % of the energy consumption impacts documented in the nine urban forms. The results highlight the prevalence of the UHI effect impacting the combined heating and cooling energy consumption of the nine building forms in Pu'er city.

Additionally, research shows that reducing the building density has a more significant influence on mitigating the UHI effect, with reductions in building height and building density leading to a decrease in heat island degree-hours (HIdh) by up to 43.7 %. Therefore, low-density buildings should be considered primarily in planning, thus alleviating the urban heat island effect and enhancing building energy efficiency in Pu'er city.

Most building layouts in Shuangyashan city, Xuzhou city, Nanjing city, and Fuzhou city exhibited a decrease in the relative change in energy demand (R) for the target buildings, with R values less than 0 for all nine neighborhood layouts. These results suggest that the energy demand of buildings surrounded by other buildings is lower than that of isolated building layouts in rural areas.

3.2. Seasonal variation of the effect of urban form on building cooling/heating energy demands

The direct and indirect influences on heating and cooling demands throughout the year depend mainly on their relative impact on winter heating demands and summer cooling demands, as well as the background climate. A seasonal assessment was adopted to understand the underlying mechanism of the overall effect. Fig. 9a and b present the R values for space cooling (summer) and heating (winter), respectively. Tables 4 and 5 depict the relative importance of direct and indirect influences, respectively, with direct impacts expressed as RID and indirect impacts expressed as RII. Table C.2 and Table C.3 (see Appendix C) presents the relative change of seasonal cooling and heating energy demands for nine different urban forms in five representative cities.

The shading effect of surrounding buildings is a significant local environmental factor affecting building energy consumption, as it reduces solar gain and thus increases heating loads in winter and decreases solar gain in summer [13,14,32,33]. In contrast, the UHI effect has a negative impact on cooling loads in summer and a positive impact on heating loads in winter due to higher ambient temperatures [34,40]. Fig. 9a depicts the distribution of the relative rates of change in summer cooling demand for the five cities under the combined effects. The findings showed that the interbuilding shading effect could have a more substantial positive impact on spatial cooling demand and reduce cooling demand in metropolises such as Shuangyashan, Xuzhou, and Fuzhou. This shows that the indirect influence of the nine urban forms is more significant, with percentages of 58 %, 60 %, and 53 %, respectively. However, in Nanjing and Pu'er, the negative influence of indirect effects on the summer cooling demand of target buildings constituted an average of 61 % and 72 %, respectively, increasing the summer cooling

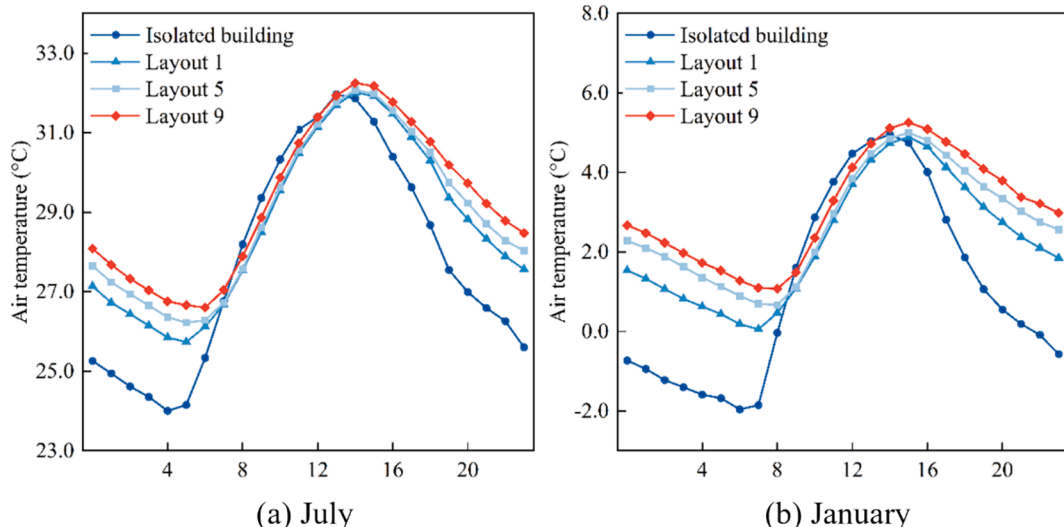


Fig. 11. Daily trend of the average outdoor temperature in Xuzhou city. (a) July (the hottest month); (b) January (the coldest month).

demand. Fig. 9b illustrates the distribution of the relative change rates for the five cities under the combined impacts. The relative importance of direct and indirect influences in winter is displayed in Table 6. In Xuzhou, Nanjing, and Fuzhou, the winter heating energy consumption of target buildings in all nine urban forms is lower than that of isolated buildings ($R < 80$). The UHI effect significantly reduced the heating load in Xuzhou, Nanjing and Fuzhou, illustrating the dominance of indirect influences. Conversely, in Pu'er city, the indirect effect (UHI) had an adverse influence on the target buildings' winter heating demand, which accounted for an average of 76 % of the combined impact, stimulating an increase in heating demand.

By analysing the seasonal cooling and heating energy demands of target buildings, we confirmed that shading from surrounding buildings increases the heating demand in winter while reducing the cooling demand in summer, contrary to the urban heat island effect. Additionally, we observed that direct and indirect impacts have varying degrees of influence on the cooling and heating energy demands of target buildings in different cities. Specifically, direct influence dominates in summer for Shuangyashan, Xuzhou, and Fuzhou, while indirect influence dominates in winter for Xuzhou, Nanjing, and Fuzhou city.

3.3. Solar heating gains through windows and urban heat island intensities in different cases

To deepen our understanding of these impacts within the studied building layout, monthly solar radiation and ambient temperature data were analysed for nine urban forms under different background climate conditions.

The shading effect of surrounding buildings is one of the most common and significant local environmental factors affecting building energy consumption [13,18]. As the density and height of buildings in a neighbourhood increase, the solar heat gain of the target building decreases due to shading by surrounding buildings. To understand the interbuilding effect, hourly data on window-transmitted solar radiation energy throughout the year were obtained for every case considered in this study. For comparison, we also calculated the solar radiation through windows of the isolated building layout. Fig. 10 shows the solar radiation per unit area of window-transmitted solar radiation (W/m^2) received by the target buildings of the nine urban forms in Xuzhou city in July (the hottest month) and January (the coldest month). The solar radiation through the window increases gradually as the altitude of the sun increases over time. At noon, when the sun reaches its highest point and has the maximum altitude angle, the solar radiation is the strongest. However, as the sun sets toward the west after noon, the altitude angle decreases, and the windowed solar radiation diminishes. Strong solar radiation may occur in the afternoon, particularly when windows face the sun. Furthermore, the window-transmitted solar radiation received by isolated buildings at different heights exhibits slight variations due to the influence of building height. This can be attributed to factors such as ground diffuse radiation, which is determined by the total solar radiation, ground reflectance, and view factor from windows to the ground [49,64]. The shading effect of surrounding buildings must be considered because it results in varying degrees of solar radiation penetrating the windows of target buildings. In general, isolated building layouts receive more window-transmitting solar radiation than do target buildings in an urban grid. The results show that the amount of window-transmitting solar radiation decreases significantly with increasing building density and height, i.e., the shading effect between buildings increases. We also find that the impact of shading was most pronounced for compact high-rise buildings, which received 90.3 % less window-transmitting solar radiation than isolated building layouts in July and 85.7 % less in January. Solar radiation from windows for different building climate zones (see Figs. D.1–D.4 in Appendix D) showed similar patterns.

The urban air temperature also plays a vital role in determining the cooling and heating energy demands of buildings. Here, Xuzhou city is taken as an example for analysis. Three geometrical forms (Layout 1:

open low-rise, Layout 5: medium density with mid-rise, and Layout 9: compact high-rise) were selected to demonstrate the impact of urban morphology on the outdoor air temperature, as shown in Fig. 11.

The results showed that air temperatures are significantly greater in compact or high layouts. Fig. 11 indicates that the rural temperature is lower than the urban temperature, apart from minor variations, and that compact high-rise buildings are the hottest. The peaks in the UHI phenomenon occur in the early morning and night, whereas the difference is small at midday. The same results apply to other cities as well. In addition, the simulation results of urban microclimate conditions demonstrate a positive correlation between the UHII and building density and height (see Table D.1 in Appendix D). Compact urban morphology has a lower sky view factor (SVF) [56], and a lower SVF will affect the loss of heat to the sky through longwave radiation from urban canyons and lead to the formation of more obvious UHIs [57]. Chen et al. [58] also proposed that street canyons with lower aspect ratios will cool more rapidly at night. In addition, compared with compact urban morphology, open urban morphology has less effect on attenuating wind speed [59], which is beneficial for heat dissipation.

4. Discussion

A great deal of research treats each building as a stand-alone entity without considering the neighboring buildings that may substantially influence energy consumption. Recent research has demonstrated that a building's energy performance is influenced by its nearby microenvironment, and the concept of IBE has been introduced and discussed within spatially proximal building layouts [37,39], as has the UHI effect. In this study, we quantified the shading effect of surrounding buildings (direct influence) and the urban heat island effect (indirect influence) on the cooling and heating energy demands of target buildings to comprehensively assess the impact of different urban microclimates on building energy demand. The research was based on nine distinctive urban morphologies in five typical cities across diverse climatic zones.

The results support that urban forms significantly modify the energy performance of buildings. For instance, in the city of Shuangyashan, heating demands dominate the annual building cooling and heating energy demands. Under the overall influence of direct and indirect effects, target buildings with open and low-rise urban morphologies exhibit lower cooling/heating energy demands. The solar heat gained through windows and the surrounding air temperature, as the fundamental causes of direct and indirect impacts, support these results. The window-transmitting solar radiation decreases significantly with increasing building density and height, i.e., the shading effect between buildings increases. We also found that high street block density and tall building height primarily cause the urban heat island effect due to the alteration of the underlying surface energy balance [36,55]. There is a positive correlation between the urban heat island intensity (UHII) and building density and height [47].

Therefore, the impact of urban form should be carefully considered in building energy simulations in urban areas. Moreover, at the stage of urban planning, the effects of urban form on building energy consumption and urban heat island intensity should be considered comprehensively.

There are several limitations in the current study. First, different building types, e.g., commercial buildings and residential buildings, often exhibit distinct energy consumption patterns [41]. The findings of this study are specific to the energy usage of residential buildings. They may not directly apply to other buildings, such as offices and retail spaces. Moreover, using idealized building forms for energy simulations while considering key driving parameters overlooks the actual building layout, physical characteristics of buildings (such as building age, user habits, and residential population), natural environment, and household economic conditions [47,65], which are essential factors determining residential building energy use. In future studies, it would be interesting to incorporate natural building morphologies to model building energy

consumption for more accurate outcomes. Second, this study considered only the indoor cooling/heating energy demands, which accounts for up to 45 % of the total energy consumption in buildings [45]. However, research has shown that natural light helps reduce the use of electric lighting and the associated sensible cooling demand caused by artificial lighting [42]. Future studies should consider these details to obtain more accurate recommendations for energy-efficient building design and urban planning strategies.

Wind speed and direction in the input weather files for Design Builder are based on rural weather stations. However, different layouts of buildings also affect the wind flow around buildings [46] and thus change the convective heat transfer coefficient, which was not considered in the present study. Regarding wind reduction and convective heat losses in urban areas, the UWG model can be further improved to generate a more realistic wind field distribution that considers site characteristics in our future studies. Furthermore, the use of natural (night) ventilation has a high potential to reduce the cooling demand of residential buildings [60,61]. Future research should focus on integrating meteorological observation stations or sophisticated computational fluid dynamics simulations of urban airflow and the impact of natural ventilation on building energy consumption. Third, this study highlights the substantial influence of shading effects caused by surrounding buildings on cooling/heating energy demands. However, the significance of external shading strategies is frequently disregarded. These shading measures possess the potential to regulate indoor daylighting and heat gain, taking into account various factors, such as season, time of day, and solar angle, ultimately influencing building energy consumption [43]. Further research is necessary to thoroughly investigate the effects of architectural shading measures on building energy consumption, as these measures can provide valuable insights for optimizing energy efficiency and reducing overall energy demand in buildings. Finally, as climate conditions continue to change, future climate patterns are expected to deviate from the current situation [44,45,71], potentially resulting in varying effects on building energy consumption across different regions. Consequently, future research must account for region-specific climate change scenarios and conduct comprehensive analyses. Considering these factors, we can improve our understanding of the potential consequences of climate conditions on building energy demand.

Nevertheless, despite the limitations mentioned above, the proposed method can effectively and objectively define a set of environmental parameters that respond to changes in the heating energy demand of buildings. The results obtained herein can not only be used to evaluate the energy efficiency of buildings but also clearly demonstrate the benefits of understanding the relationship between the energy demand of a building and its surroundings.

5. Conclusions

The impacts of shading from surrounding buildings and the urban heat island effect on the energy performance of buildings under different climatic conditions are quantitatively evaluated and analysed in this study. A comprehensive framework for modelling and quantifying is established. The validated UWG model was used to simulate the UHI intensities in different urban forms. Nine building layouts ranging from high-rise compact to low-rise open forms were compared with isolated buildings. The inter-building effects were considered based on the validated building energy simulation models. The space cooling and heating energy demands for an isolated building and a target building

located in different urban forms are compared in five typical cities in five representative building climate zones of China.

The two main influencing mechanisms of urban form are identified as (i) direct influence due to the blocking of solar/longwave radiation and (ii) indirect influence due to the urban heat island effect induced by different urban forms.

The results showed that the overall effect of urban form on annual building demands depended on the background climate. In Shuangyashan city (a cold region), the yearly demand is lowest in open low-rise layouts and 3.1 % less than that in isolated building layouts due to direct and indirect influences. The compact high-rise buildings in Pu'er (a mild area) have an annual demand 29.5 % higher than that of the isolated building layout. Indirect influence was responsible for an average of 85 % of the energy consumption impacts documented in the nine urban forms in Pu'er. However, Xuzhou city (cold region) and Nanjing city (hot summer and cold winter region) favor compact high-rise building forms (2.8 % lower) and compact low-rise building forms (3.3 % lower), respectively. For Xuzhou city, the average share of indirect impacts under the nine neighborhood layouts is 80 % throughout the year. However, the results for winter and summer show that direct influence dominates in summer at 60 %, and indirect impacts dominate in winter at 59. In Nanjing, the proportion of indirect influence on the energy consumption of the target buildings under the different layout types reaches 74, which indicates that the IBE effect significantly affects the energy performance of the buildings in Nanjing.

Understanding the distinct influences of the IBE and UHI effects could lead to the optimization of the thermal energy performance within spatially proximal buildings. Urbanization will become increasingly crucial as it will rapidly create dense urban environments in cities worldwide.

CRediT authorship contribution statement

Yiman Zhao: Writing – original draft, Validation, Software, Methodology, Conceptualization. **Xiaotian Ding:** Writing – original draft, Validation, Software, Methodology, Conceptualization. **Ziyu Wu:** Visualization, Validation, Software, Formal analysis, Conceptualization. **Shi Yin:** Writing – review & editing, Visualization, Resources, Formal analysis. **Yifan Fan:** Writing – review & editing, Validation, Supervision, Resources, Formal analysis, Conceptualization. **Jian Ge:** Writing – review & editing, Supervision, Resources, Formal analysis.

Declaration of competing interest

The authors declare that they have no known competing financial interests or personal relationships that could have appeared to influence the work reported in this paper.

Data availability

Data will be made available on request.

Acknowledgements

This research was funded by the “Pioneer” and “Leading Goose” R&D Program of Zhejiang (2023C03152), the National Natural Science Foundation of China (No. 52208130) and the Zhejiang Provincial Natural Science Foundation of China (No. LQ21E080014).

Appendix A

The climatic characteristics of the cities, represented by the five building climate zones and the typical layouts of the residential buildings.

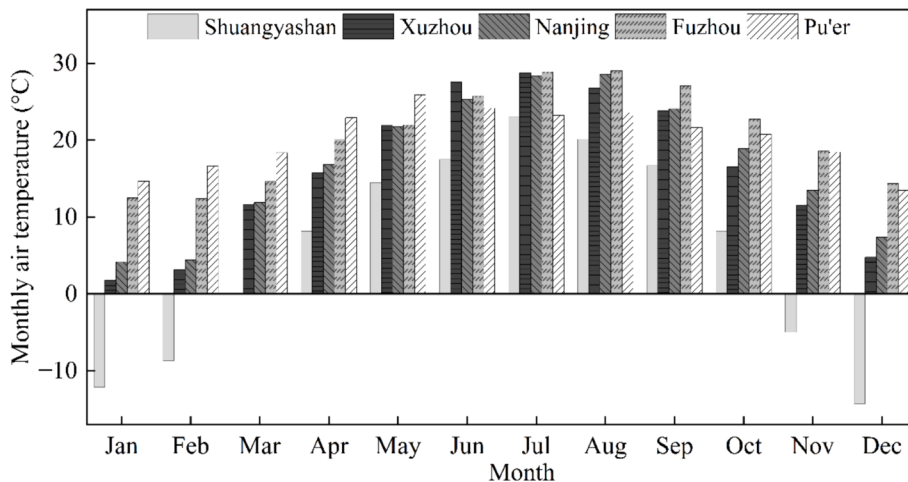


Fig. A1. Monthly average temperature for five representative cities in 2019.

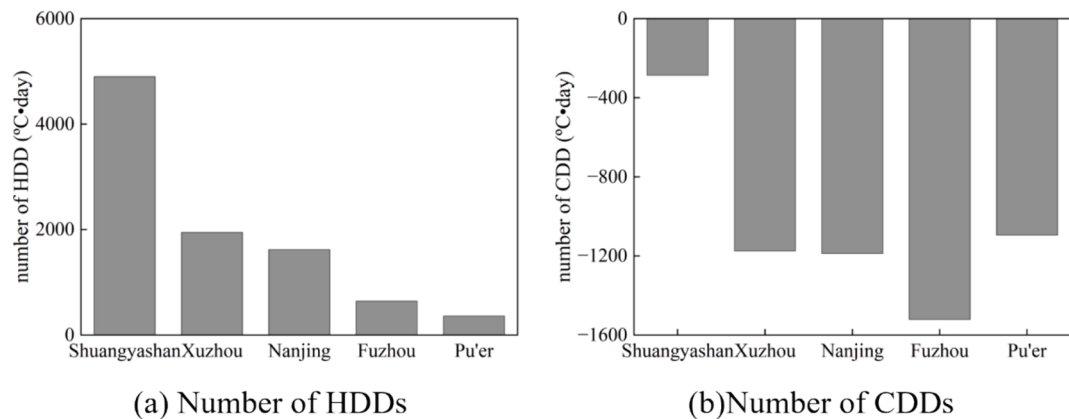
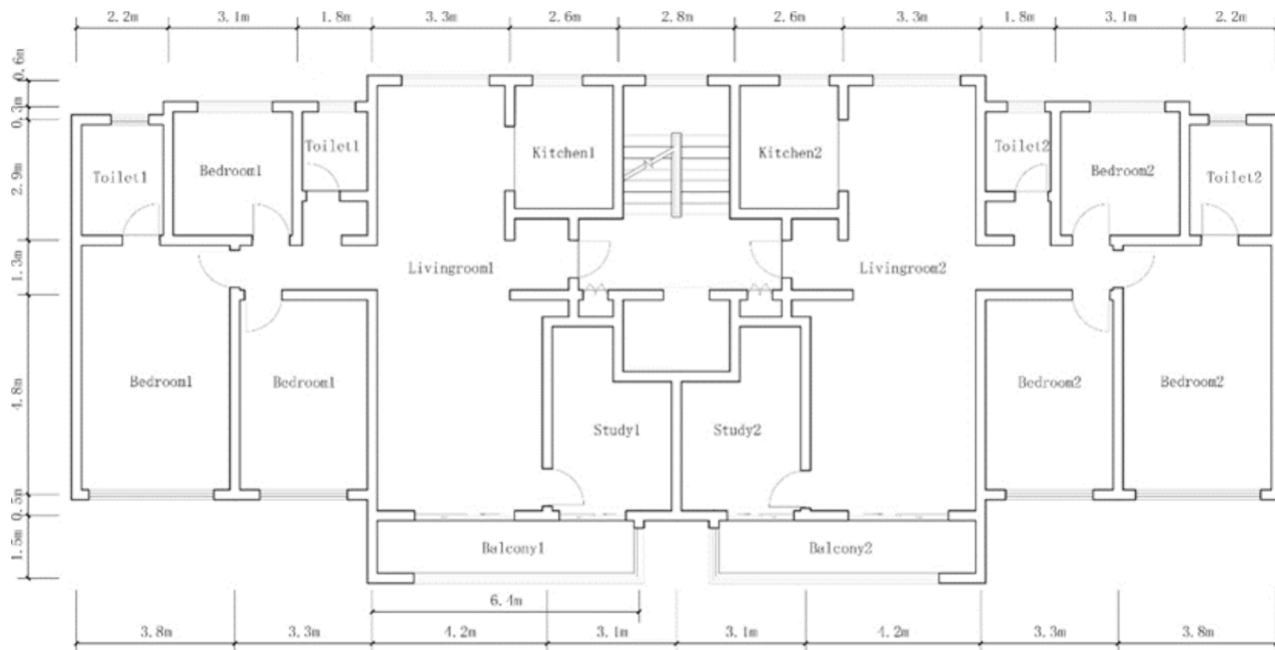
Fig. A2. Heating and cooling degree days for five representative cities in 2019 (base temperature: 18 $^{\circ}\text{C}$): (a) Number of HDD, (b) Number of CDD.

Fig. A3. Layout and geometric parameters of the simulated typical residential building [30].

Table A1

The hourly occupancy or utilization rate of occupancy, equipment, and lighting for different room types.

Room type	Energetic behavior	Time											
		1	2	3	4	5	6	7	8	9	10	11	12
Bedroom	occupancy	100	100	100	100	100	100	50	50	0	0	0	0
	Equipment	0	0	0	0	0	0	100	100	0	0	0	0
	Lighting	0	0	0	0	0	100	50	0	0	0	0	0
Living room	occupancy	0	0	0	0	0	0	50	50	100	100	100	100
	Equipment	0	0	0	0	0	0	50	100	100	50	50	100
	Lighting	0	0	0	0	0	50	100	0	0	0	0	0
Kitchen	occupancy	0	0	0	0	0	0	100	0	0	0	0	100
	Equipment	0	0	0	0	0	0	100	0	0	0	0	100
	Lighting	0	0	0	0	0	0	100	0	0	0	0	0
Toilet	occupancy	0	0	0	0	0	50	50	10	10	10	10	10
	Equipment	0	0	0	0	0	0	0	0	0	0	0	0
	Lighting	0	0	0	0	0	50	50	10	10	10	10	10
Study room	occupancy	0	0	0	0	0	10	10	10	10	10	10	10
	Equipment	0	0	0	0	0	0	0	0	0	0	0	0
	Lighting	0	0	0	0	0	10	10	10	10	10	10	10
Time													
Room type	Energetic behavior	13	14	15	16	17	18	19	20	21	22	23	24
Bedroom	occupancy	0	0	0	0	0	0	0	0	50	100	100	100
	Equipment	0	0	0	0	0	0	0	0	100	100	0	0
	Lighting	0	0	0	0	0	0	0	0	100	100	0	0
Living room	occupancy	100	100	100	100	100	100	100	100	50	0	0	0
	Equipment	100	50	50	50	50	100	100	100	50	0	0	0
	Lighting	0	0	0	0	0	0	100	100	50	0	0	0
Kitchen	occupancy	0	0	0	0	0	100	0	0	0	0	0	100
	Equipment	0	0	0	0	0	100	0	0	0	0	0	100
	Lighting	0	0	0	0	0	100	0	0	0	0	0	0
Toilet	occupancy	10	10	10	10	10	10	10	50	50	0	0	0
	Equipment	0	0	0	0	0	0	0	0	0	0	0	0
	Lighting	10	10	10	10	10	10	10	50	50	0	0	0
Study room	occupancy	10	10	10	10	10	10	10	10	10	0	0	0
	Equipment	0	0	0	0	0	0	0	0	0	0	0	0
	Lighting	10	10	10	10	10	10	10	10	10	0	0	0

Table A2

Different types of room areas and air conditioning settings.

	Area (m ²)	Area ratio (%)	Air conditioning
Living room	40.8	36.4	yes
Bedroom	39.8	35.5	yes
Kitchen	6.5	6.4	no
Toilet	7.4	6.6	no
Study room	9.8	8.8	yes
Balcony	7.7	6.3	no
Staircase	—	—	no

Table A3
Actual cooling and heating period of five representative cities.

Region	Represent city	Cooling period	Heating period
1	Shuangyashan	24 Jun – 10 Nov	17 Nov – 24 May
2	Xuzhou	10 May – 5 Oct	16 Oct – 30 Apr
3	Nanjing	22 May – 25 Sep	2 Nov – 4 May
4	Fuzhou	21 Apr – 4 Nov	28 Nov – 16 Apr
5	Pu'er	6 Apr – 24 Oct	28 Nov – 26 Mar

Appendix B

Validation of UWG site pair locations and urban form parameters, as well as building energy models.



Fig. B1. Locations of urban ($26^{\circ}05' N$, $119^{\circ}17' E$) and rural ($26^{\circ}30' N$, $119^{\circ}33' E$) weather stations in Fuzhou city (Google Earth v7.3.4.8428, Google Inc, United States).

Table B1
Location information of weather stations.

ID number	Name	Latitude	Longitude	Elevation (m)
58,847	Fuzhou	$26^{\circ}05'00'' N$	$119^{\circ}17'00'' E$	84.1
58,845	Luoyuan	$26^{\circ}30'00'' N$	$119^{\circ}33'00'' E$	78.8

Table B2

The urban parameters within a 500 m buffer zone around the urban weather station in Fuzhou city.

Average building height (m)	Average Building density	Facade to site ratio	Tree cover	Grass cover
18.39	0.33	4.17	28	2

Table B3

The monthly and annual root mean square errors (RMSEs) of hourly temperatures at Fuzhou weather stations with simulated hourly temperatures at the city weather generator.

Month	RMSE (K)
January	1.64
February	1.13
March	1.02
April	1.70
May	1.29
June	1.09
July	1.41
August	1.27
September	1.84
October	0.98

(continued on next page)

Table B3 (continued)

Month	RMSE (K)
November	1.60
December	1.53
Annual	1.37

**Fig. B2.** A 3D building model was used for validation of building energy consumption modelling [22].**Fig. B3.** Locations of the zero-energy building ($38^{\circ}0' N$, $78^{\circ}29' E$) and rural ($38^{\circ}6' N$, $78^{\circ}26' E$) weather station in Charlottesville, Virginia, USA (Google Earth v7.3.4.8428, Google Inc, United States).**Table B4**

The urban parameters within a 500-meter buffer zone around the zero-energy building in Charlottesville, Virginia, USA.

Average building height (m)	Average Building density	Facade to site ratio	Tree cover	Grass cover
7.32	0.09	2.98	68	8

Appendix C

The relative change in the R of the annual and seasonal cooling/heating energy demands for cities represents five climate zones in China.

Table C1

1. The actual heating and cooling demand and the rate of change compared to isolated buildings of 9 layouts in Shuangyashan city.

Urban form	Heating demand (kW/m^2)			Cooling demand (kW/m^2)			Annual R (%)
	$E_{\text{baseline scenario}}$	$E_{\text{Scenario C}}$	$R_{\text{heating}} (\%)$	$E_{\text{baseline scenario}}$	$E_{\text{Scenario C}}$	$R_{\text{cooling}} (\%)$	
Layout 1	121.9	118.1	-3.2	4.9	4.9	-0.5	-3.1
Layout 2	121.9	120.1	-1.5	4.9	4.4	-10.6	-1.9
Layout 3	121.9	122	0.1	4.9	3.9	-21	-0.7
Layout 4	118	117.1	-0.8	5.3	4.6	-11.8	-1.2
Layout 5	118	118.9	0.8	5.3	4.2	-20.9	-0.2
Layout 6	118	120.1	1.8	5.3	3.8	-28.3	0.6
Layout 7	132.8	133.3	0.4	5.9	4.7	-21.4	-0.6
Layout 8	132.8	134.6	1.3	5.9	4.3	-27.9	0.1
Layout 9	132.8	135	1.6	5.9	4.1	-30.5	0.3

Table C1

2. The actual heating and cooling demand and the rate of change compared to isolated buildings of 9 layouts in Xuzhou city.

Urban form	Heating demand (kW/m^2)			Cooling demand (kW/m^2)			Annual R (%)
	$E_{\text{baseline scenario}}$	$E_{\text{Scenario C}}$	$R_{\text{heating}} (\%)$	$E_{\text{baseline scenario}}$	$E_{\text{Scenario C}}$	$R_{\text{cooling}} (\%)$	
Layout 1	45.7	41.9	-8.3	30.6	31.9	4.5	-3.2
Layout 2	45.7	42.8	-6.3	30.6	30.5	-0.1	-3.8
Layout 3	45.7	44	-3.8	30.6	29	-5.2	-4.4
Layout 4	42.3	40.6	-4	30.1	30.9	2.6	-1.3
Layout 5	42.3	41.6	-1.8	30.1	29.4	-2.3	-2
Layout 6	42.3	42.3	-0.1	30.1	28.3	-6.1	-2.6
Layout 7	42.6	40.6	-4.7	31	29.9	-3.6	-4.3
Layout 8	42.6	41.3	-3.1	31	28.8	-7.2	-4.8
Layout 9	42.6	41.6	-2.4	31	28.2	-9	-5.2

Table C1

3. The actual heating and cooling demand and the rate of change compared to isolated buildings of 9 layouts in Nanjing city.

Urban form	Heating demand (kW/m^2)			Cooling demand (kW/m^2)			Annual R (%)
	$E_{\text{baseline scenario}}$	$E_{\text{Scenario C}}$	$R_{\text{heating}} (\%)$	$E_{\text{baseline scenario}}$	$E_{\text{Scenario C}}$	$R_{\text{cooling}} (\%)$	
Layout 1	81.2	71.6	-11.8	37.3	42.4	13.6	-3.8
Layout 2	81.2	72.6	-10.7	37.3	41.3	10.7	-3.9
Layout 3	81.2	73.7	-9.3	37.3	39.9	6.8	-4.2
Layout 4	78.4	70.1	-10.7	37.1	41.6	12	-3.4
Layout 5	78.4	71.0	-9.4	37.1	40.5	9.1	-3.5
Layout 6	78.4	71.5	-8.9	37.1	40.1	7.9	-3.5
Layout 7	78.1	69.4	-11.1	36.5	41.3	13.3	-3.3
Layout 8	78.1	69.9	-10.5	36.5	40.8	11.9	-3.4
Layout 9	78.1	69.7	-10.7	36.5	40.7	11.7	-3.5

Table C1

4. The actual heating and cooling demand and the rate of change compared to isolated buildings of 9 layouts in Fuzhou city.

Urban form	Heating demand (kW/m^2)			Cooling demand (kW/m^2)			Annual R (%)
	$E_{\text{baseline scenario}}$	$E_{\text{Scenario C}}$	$R_{\text{heating}} (\%)$	$E_{\text{baseline scenario}}$	$E_{\text{Scenario C}}$	$R_{\text{cooling}} (\%)$	
Layout 1	29.8	26.3	-11.9	64.6	67.1	3.9	-1.1
Layout 2	29.8	26.4	-11.5	64.6	66.3	2.6	-1.8
Layout 3	29.8	26.7	-10.4	64.6	64.7	0	-3.3
Layout 4	27.8	24.7	-11.3	63.2	65.2	3.3	-1.2
Layout 5	27.8	24.9	-10.3	63.2	64	1.3	-2.3
Layout 6	27.8	25.2	-9.5	63.2	62.9	-0.5	-3.2
Layout 7	27.6	24.4	-11.5	61.8	63.7	3	-1.5
Layout 8	27.6	24.5	-11.3	61.8	63.1	2.1	-2.1
Layout 9	27.6	24.3	-11.9	61.8	63.5	2.6	-1.9

Table C1

5. The actual heating and cooling demand and the rate of change compared to isolated buildings of 9 layouts in Pu'er city.

Urban form	Heating demand (kW/m ²)			Cooling demand (kW/m ²)			Annual R (%)
	E _{baseline scenario}	E _{Scenario C}	R _{heating (%)}	E _{baseline scenario}	E _{Scenario C}	R _{cooling (%)}	
Layout 1	14.2	12.2	-14.0	53.9	71.4	32.6	22.9
Layout 2	14.2	12.8	-9.8	53.9	70.3	30.5	22.1
Layout 3	14.2	13.9	-2.5	53.9	68.7	27.6	21.3
Layout 4	13.3	13.7	3.0	56.6	71.7	26.7	22.2
Layout 5	13.3	14.9	11.9	56.6	71.3	25.9	23.3
Layout 6	13.3	15.9	19.5	56.6	71	25.5	24.3
Layout 7	13.8	15.6	12.6	55.7	72.5	30.2	26.7
Layout 8	13.8	16.6	19.9	55.7	72.2	29.8	27.8
Layout 9	13.8	17.1	23.6	55.7	72.9	30.9	29.5

Table C2

The relative change in the R of the annual cooling/heating energy demands for cities represents five climate zones in China.

		Shuangyashan (%)	Xuzhou (%)	Nanjing (%)	Fuzhou (%)	Pu'er (%)
Layout 1	Scenario A	2.4	-2.1	-1.3	-4.1	-2.8
	Scenario B	-5.1	-0.6	-2.1	3.1	29.1
	Scenario C	-3.1	-3.2	-3.8	-1.1	22.9
Layout 2	Scenario A	4.0	-2.4	-1.2	-5.6	-4.3
	Scenario B	-5.3	-0.6	-2.0	3.8	30.0
	Scenario C	-1.9	-3.8	-3.9	-1.8	22.1
Layout 3	Scenario A	5.6	-2.6	-1.2	-7.4	-5.5
	Scenario B	-5.5	-0.6	-2.1	4.3	33.1
	Scenario C	-0.7	-4.4	-4.2	-3.3	21.3
Layout 4	Scenario A	5.4	-1.9	-0.5	-5.9	-5.8
	Scenario B	-5.9	-0.7	-2.1	4.9	29.2
	Scenario C	-1.2	-3.7	-3.4	-1.2	22.2
Layout 5	Scenario A	7.0	-2.2	-0.3	-7.7	-6.8
	Scenario B	-6.1	-0.7	-2.0	5.6	31.7
	Scenario C	-0.2	-4.5	-3.5	-2.3	23.3
Layout 6	Scenario A	8.4	-2.5	-0.4	-9.4	-7.7
	Scenario B	-6.4	-0.6	-1.6	6.5	34.1
	Scenario C	0.6	-5.0	-3.5	-3.2	24.3
Layout 7	Scenario A	7.3	-2.0	-0.3	-7.52	-5.9
	Scenario B	-6.8	-0.6	-1.8	6.3	34.4
	Scenario C	-0.6	-4.3	-3.3	-1.5	26.7
Layout 8	Scenario A	8.8	-2.3	-0.2	-9.20	-7.0
	Scenario B	-7.2	-0.4	-1.6	7.5	37.1
	Scenario C	0.1	-4.8	-3.4	-2.1	27.8
Layout 9	Scenario A	9.7	-2.8	-4.8	-10.4	-7.7
	Scenario B	-7.7	-0.3	-5.8	9.0	40.1
	Scenario C	0.3	-5.2	-3.5	-1.9	29.5

Note: Scenario A focuses on the simulation process and considers only direct influence; Scenario B focuses on the simulation process and considers only indirect influence; Scenario C incorporates both direct and indirect influences.

Table C3

The relative change in the R value of the cooling demand in summer for cities represents five climate zones in China.

		Shuangyashan (%)	Xuzhou (%)	Nanjing (%)	Fuzhou (%)	Pu'er (%)
Layout 1	Scenario A	-26.2	-10.6	-8.4	-6.3	-3.2
	Scenario B	27.0	11.1	20.3	7.4	25.9
	Scenario C	-2.3	1.1	11.9	1.3	19.9
Layout 2	Scenario A	-35.9	-15.3	-11.9	-8.8	-5.8
	Scenario B	28.3	11.6	21.1	8.5	26.9
	Scenario C	-11.8	-2.9	9.5	0.1	18.7
Layout 3	Scenario A	-45.9	-20.6	-16.4	-12.0	-9.3
	Scenario B	29.9	12.1	21.5	9.2	28.0
	Scenario C	-21.4	-7.3	6.0	-2.2	17.1
Layout 4	Scenario A	-38.2	-13.5	-13.6	-10.2	-10.5
	Scenario B	29.9	17.2	23.3	9.8	24.9
	Scenario C	-13.0	-3.4	10.6	0.2	16.4
Layout 5	Scenario A	-47.5	-19.0	-17.7	-13.4	-13.9
	Scenario B	32.2	18.0	24.4	10.9	27.2
	Scenario C	-21.2	-7.4	8.2	-1.7	16.3
Layout 6	Scenario A	-55.3	-23.6	-20.8	-16.3	-16.9
	Scenario B	34.7	19.0	26.9	12.2	29.5
	Scenario C	-28.0	-10.5	7.5	-3.1	16.5
Layout 7	Scenario A	-49.0	-21.9	-17.2	-13.3	-13.5
	Scenario B	33.5	14.3	28.1	12.2	29.7
	Scenario C	-21.3	-6.1	12.1	-0.3	19.3
Layout 8	Scenario A	-57.5	-26.9	-20.9	-16.4	-16.9
	Scenario B	37.5	15.5	30.4	14.0	32.1
	Scenario C	-27.4	-9.2	11.0	-1.2	19.3
Layout 9	Scenario A	-62.9	-30.4	-23.5	-18.5	-19.2
	Scenario B	42.1	16.9	33.0	16.1	34.6
	Scenario C	-29.9	-10.8	10.8	-0.9	20.4

Note: Scenario A focuses on the simulation process and considers only direct influence; Scenario B focuses on the simulation process and considers only indirect influence; Scenario C incorporates both direct and indirect influences.

Table C4

The relative change in the R of heating demand in winter for cities represents five climate zones in China.

		Shuangyashan (%)	Xuzhou (%)	Nanjing (%)	Fuzhou (%)	Pu'er (%)
Layout 1	Scenario A	2.9	3.4	1.7	1.8	42.1
	Scenario B	-4.7	-10.0	-9.8	-14.4	-6.3
	Scenario C	-1.9	-6.8	-8.3	-12.9	4.9
Layout 2	Scenario A	4.5	5.9	3.3	3.3	55.5
	Scenario B	-5.0	-10.6	-10.3	-14.9	-7.0
	Scenario C	-0.7	-5.0	-7.2	-12.1	13.7
Layout 3	Scenario A	5.6	8.5	4.9	5.8	77.9
	Scenario B	-5.3	-11.0	-10.6	-15.4	14.4
	Scenario C	0.1	-2.9	-6.1	-10.5	28.8
Layout 4	Scenario A	5.5	10.8	5.0	6.5	42.1
	Scenario B	-5.6	-10.9	-11.7	-16.9	-26.3
	Scenario C	-0.2	-4.9	-7.1	-11.3	3.3
Layout 5	Scenario A	6.7	13.4	6.6	9.1	61.6
	Scenario B	-6.0	-11.6	-12.1	-17.8	-27.2
	Scenario C	0.5	-3.3	-6.2	-9.9	16.5
Layout 6	Scenario A	7.5	15.3	7.5	11.7	78.1

(continued on next page)

Table C4 (continued)

		Shuangyashan (%)	Xuzhou (%)	Nanjing (%)	Fuzhou (%)	Pu'er (%)
	Scenario B	-6.4	-12.3	-12.8	-18.8	-28.4
	Scenario C	0.9	-2.2	-6.0	-8.8	26.9
Layout 7	Scenario A	6.7	11.2	6.3	9.9	63.5
	Scenario B	-6.5	-14.6	-13.5	-19.5	-27.5
	Scenario C	0.0	-4.2	-7.7	-11.0	17.3
Layout 8	Scenario A	7.7	13.4	7.6	12.2	80.4
	Scenario B	-7.2	-15.6	-14.4	-21.0	-29.1
	Scenario C	0.3	-3.2	-7.4	-10.6	27.2
Layout 9	Scenario A	8.3	9.5	6.1	13.9	91.4
	Scenario B	-7.9	-21.8	-17.6	-22.8	-30.9
	Scenario C	0.1	-2.9	-7.7	-11.1	32.2

Note: Scenario A focuses on the simulation process and considers only direct influence; Scenario B focuses on the simulation process and considers only indirect influence; Scenario C incorporates both direct and indirect influences.

Appendix D

Daily trends in average solar heat gain through windows and daily trends in the average outdoor temperature during the hottest and coldest months for target buildings of different building forms in five representative cities.

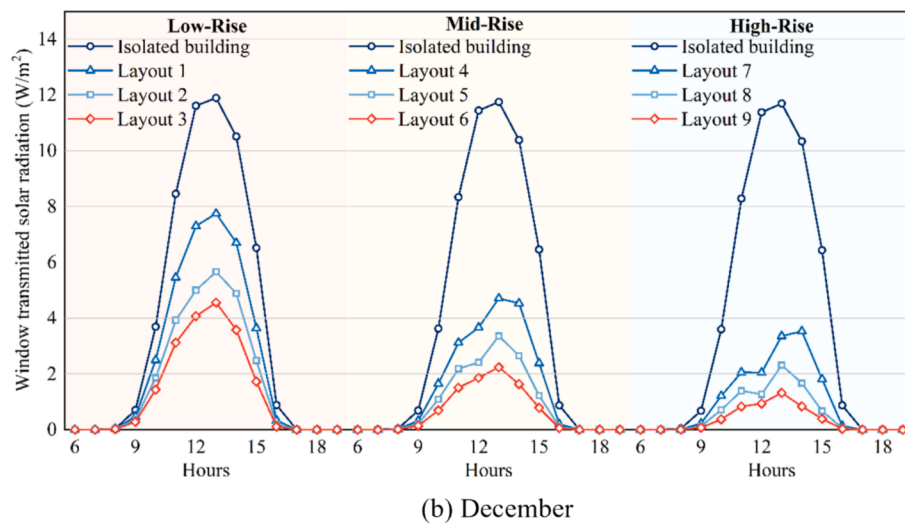
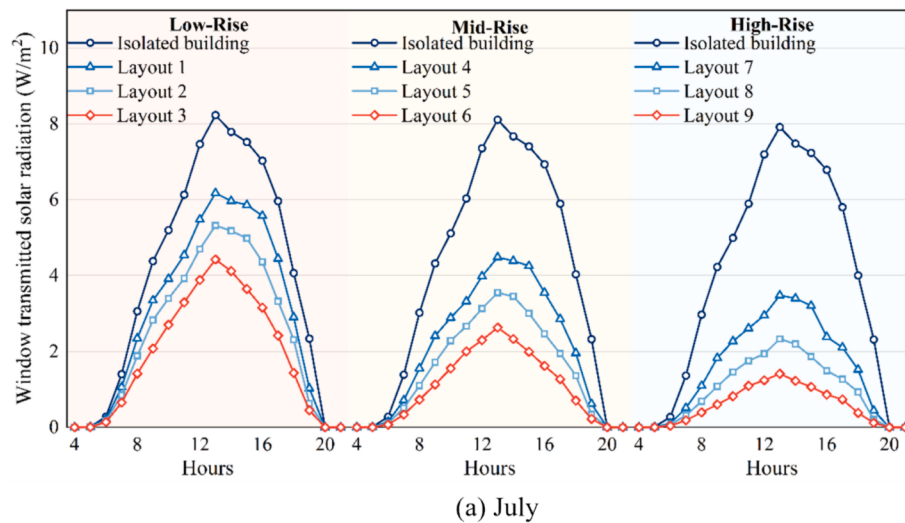


Fig. D1. Daily trends in average solar heat gain through windows in Shuangyashan city in (a) July (the hottest month) and (b) December (the coldest month).

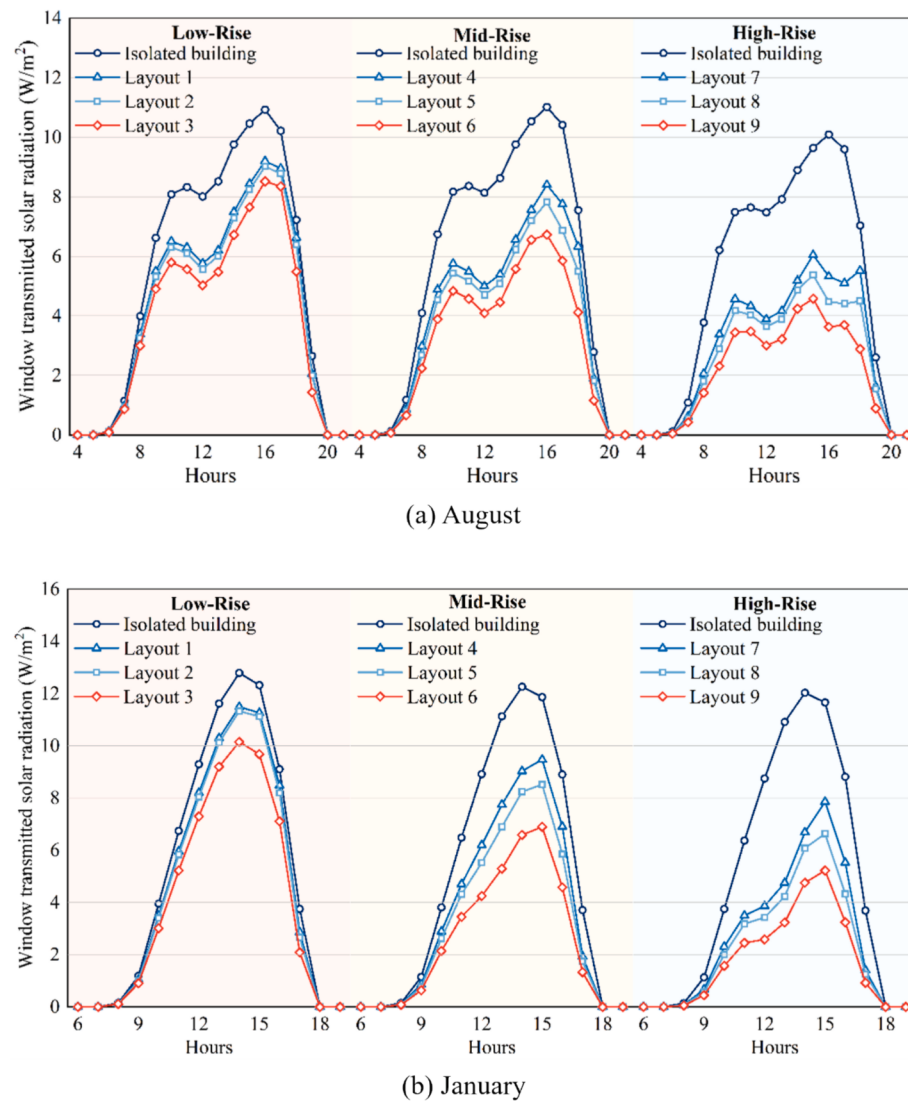


Fig. D2. Daily trends in average solar heat gain through windows in Nanjing city. (a) August (the hottest month); (b) January (the coldest month).

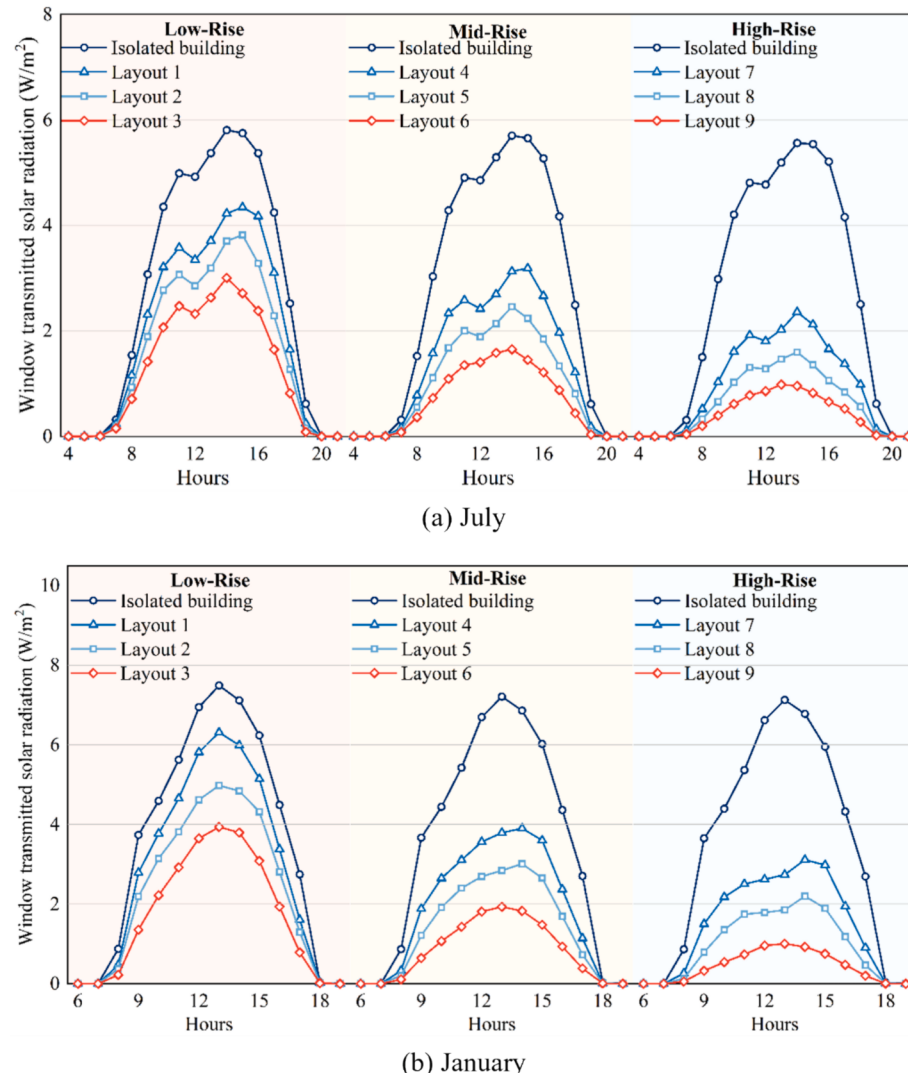
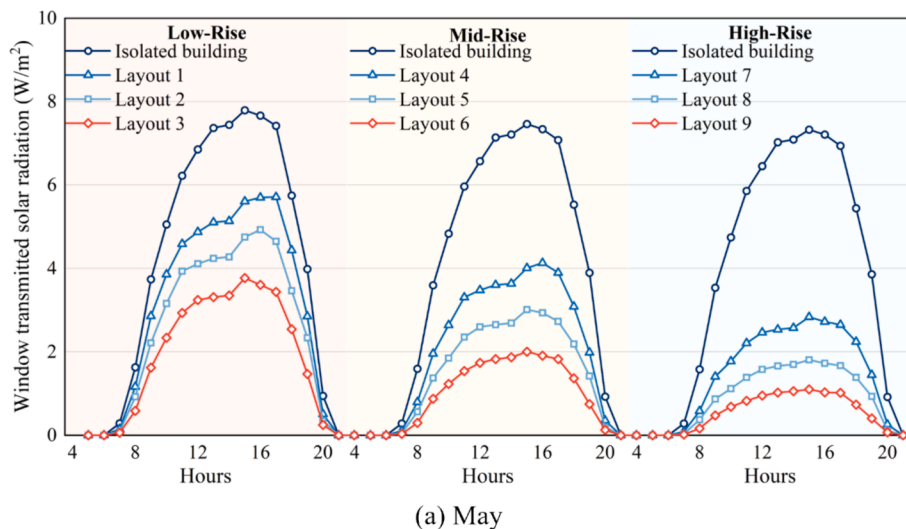
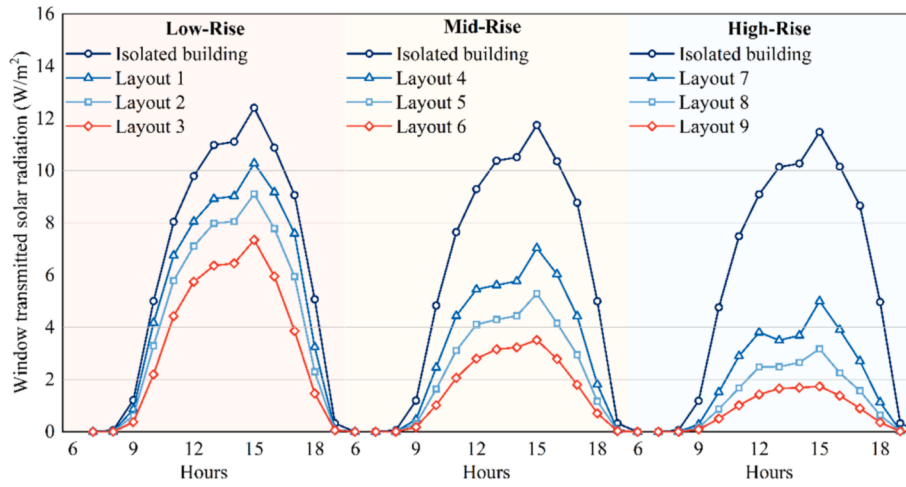


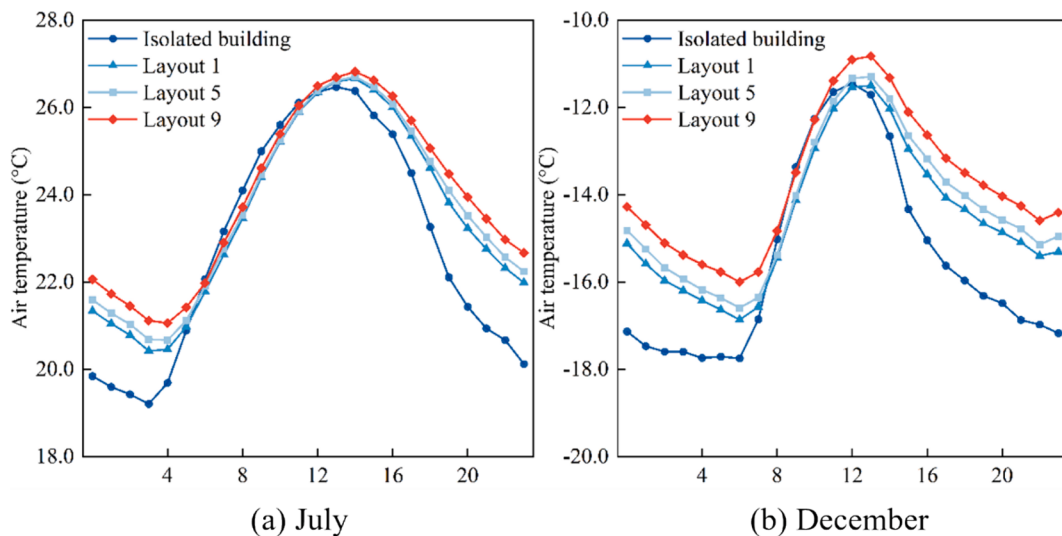
Fig. D3. Daily trends in average solar heat gain through windows in Fuzhou city. (a) July (the hottest month); (b) January (the coldest month).



(a) May



(b) December

Fig. D4. Daily trends in average solar heat gain through windows in Pu'er city. (a) July (the hottest month); (b) December (the coldest month).**Fig. D5.** Daily trend of the average outdoor temperature in Shuangyashan city. (a) July (the hottest month); (b) December (the coldest month).

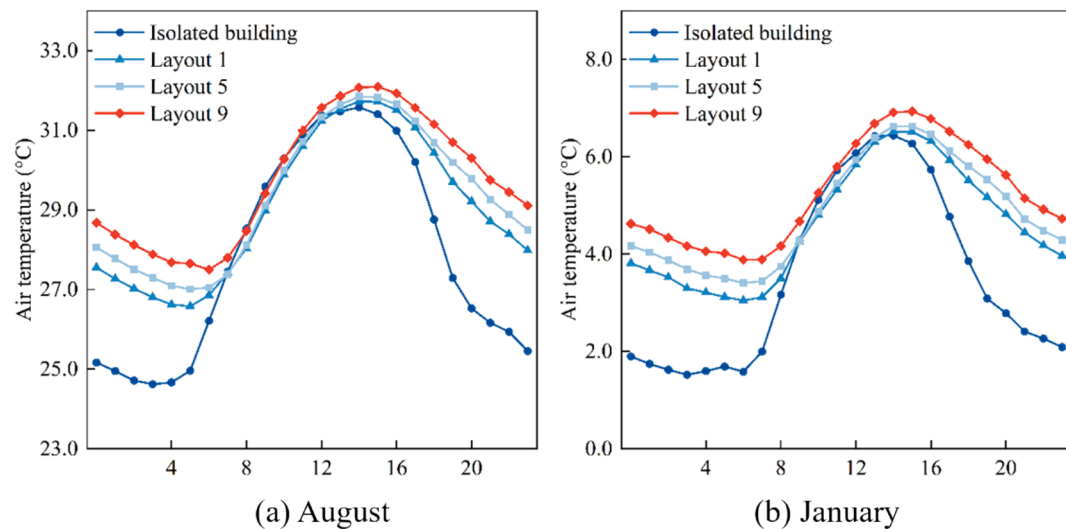


Fig. D6. Daily trend of average outdoor temperature in Nanjing city. (a) August (the hottest month); (b) January (the coldest month).

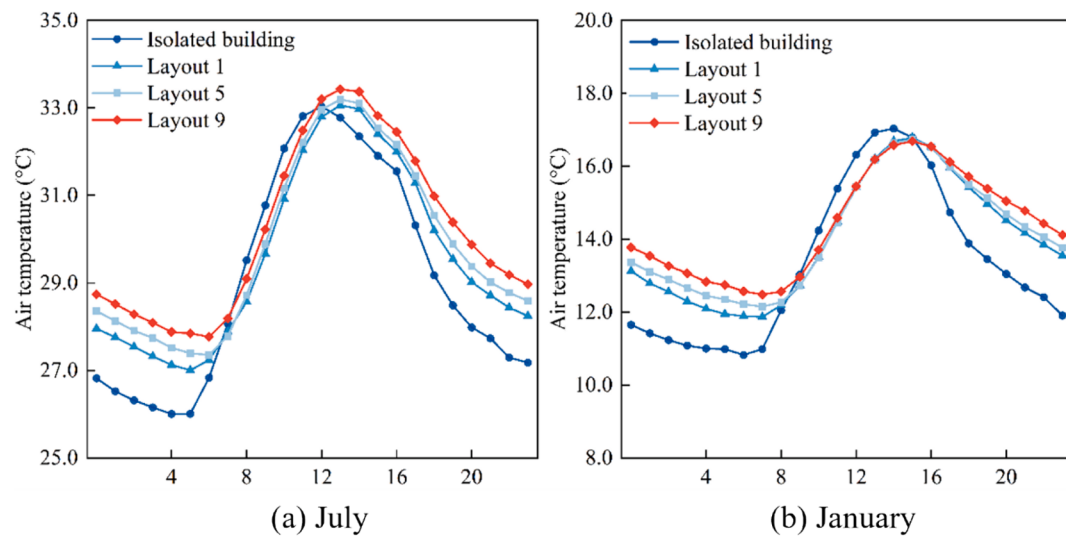


Fig. D7. Daily trend of average outdoor temperature in Fuzhou city. (a) July (the hottest month); (b) January (the coldest month).

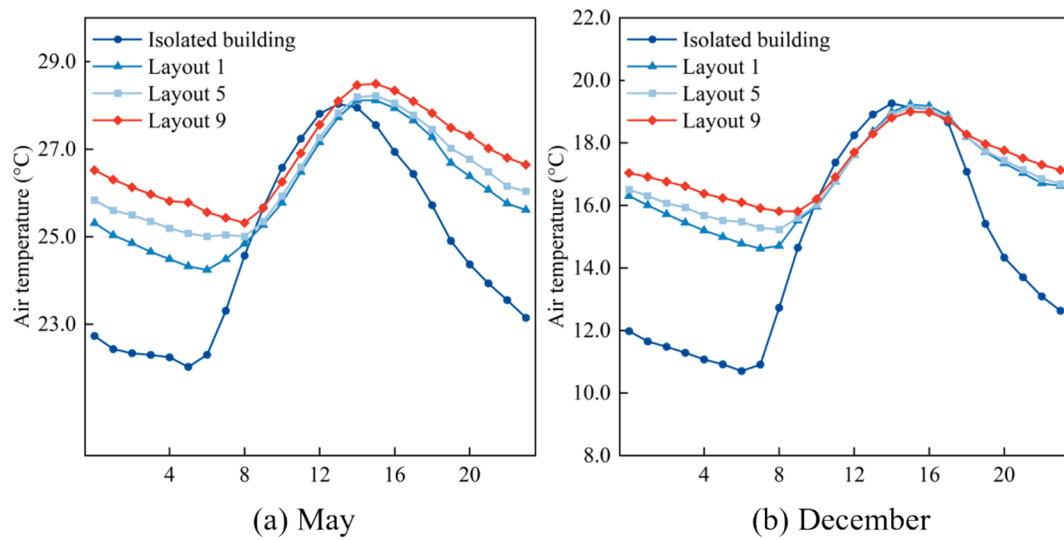


Fig. D8. Daily trend of average outdoor temperature in Pu'er city. (a) May (the hottest month); (b) December (the coldest month).

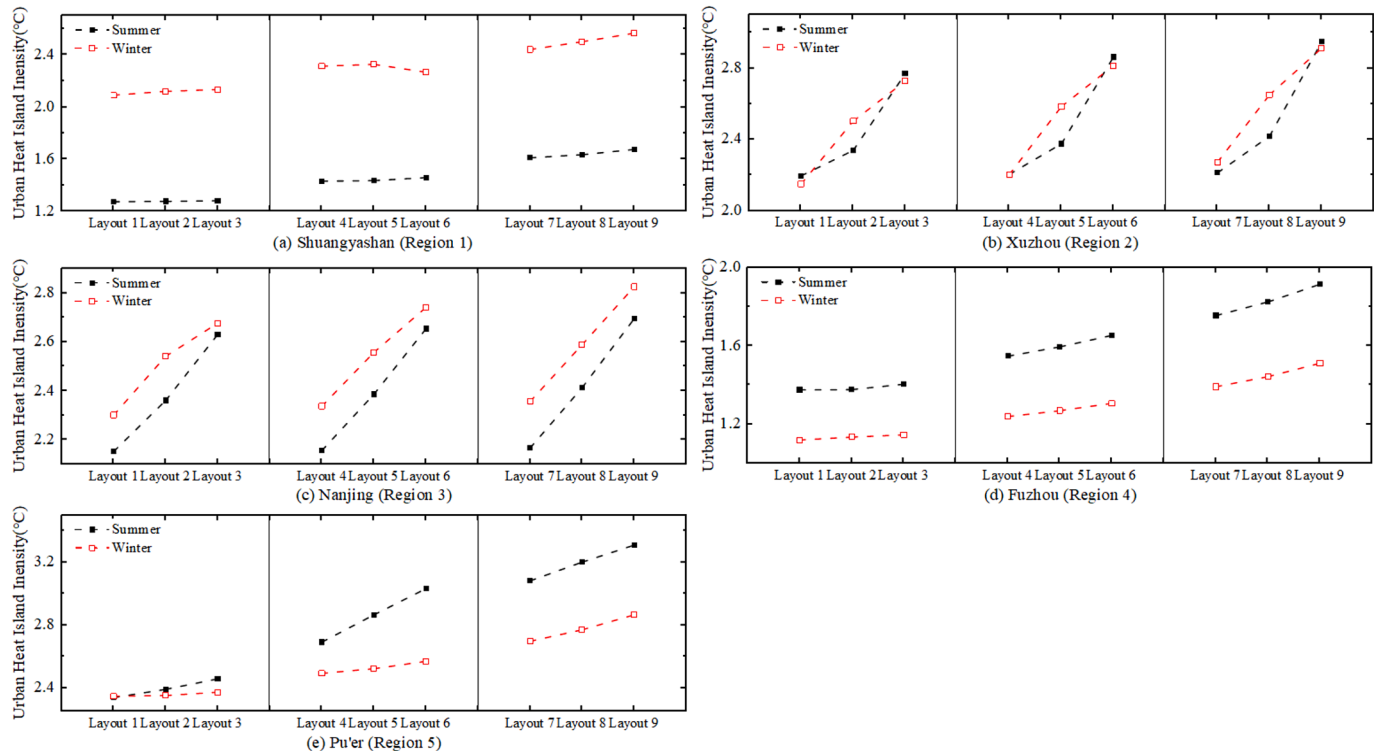


Fig. D9. Trends in winter/summer heat island intensity with building height for representative cities in different building climate zones for three sets of building densities.

Table D1

Urban heat island intensity under different combinations of building density and height in Fuzhou city in summer and winter.

	0.25	0.30	0.35	0.40	0.45	0.50
Summer						
9 m	0.59	0.62	0.68	0.71	0.72	0.73
15 m	0.66	0.69	0.72	0.75	0.79	0.83
21 m	0.74	0.75	0.79	0.83	0.88	0.93
27 m	0.76	0.80	0.84	0.89	0.95	1.01
33 m	0.79	0.84	0.89	0.94	1.00	1.07
39 m	0.82	0.87	0.93	0.98	1.05	1.12
45 m	0.84	0.90	0.96	1.02	1.09	1.17

(continued on next page)

Table D1 (continued)

	0.25	0.30	0.35	0.40	0.45	0.50
51 m	0.87	0.93	0.99	1.06	1.13	1.22
Winter						
9 m	0.71	0.71	0.73	0.73	0.75	0.76
15 m	0.71	0.72	0.73	0.75	0.76	0.79
21 m	0.74	0.76	0.77	0.79	0.81	0.84
27 m	0.76	0.78	0.80	0.82	0.84	0.87
33 m	0.78	0.80	0.82	0.85	0.88	0.91
39 m	0.80	0.82	0.84	0.87	0.90	0.94
45 m	0.81	0.83	0.86	0.89	0.92	0.96
51 m	0.82	0.85	0.87	0.91	0.95	0.99

References

- [1] M. González-Torres, L. Pérez-Lombard, J.F. Coronel, I.R. Maestre, D. Yan, A review on buildings energy information: trends, end-uses, fuels and drivers, *Energy Rep.* 8 (2022) 626–637.
- [2] Y. Chen, T. Hong, Impacts of building geometry modelling methods on the simulation results of urban building energy models, *Appl. Energy* 215 (2018) 717–735.
- [3] Y. Fan, Y. Li, A. Bejan, Y. Wang, X. Yang, Horizontal extent of the urban heat dome flow, *Sci. Rep.* 7 (1) (2017) 11681.
- [4] Y. Fan, Q. Wang, S. Yin, Y. Li, Effect of city shape on urban wind patterns and convective heat transfer in calm and stable background conditions, *Build. Environ.* 162 (2019) 106288.
- [5] X. Ding, Y. Zhao, Y. Fan, Y. Li, J. Ge, Machine learning-assisted mapping of city-scale air temperature: Using sparse meteorological data for urban climate modelling and adaptation, *Build. Environ.* 234 (2023) 110211.
- [6] Y. Zhang, X. Wang, Y. Fan, Y. Zhao, J. Carmeliet, J. Ge, Urban heat dome flow deflected by the Coriolis force, *Urban Clim.* 49 (2023) 101449.
- [7] R. Ourghi, A. Al-Anzi, M. Krarti, A simplified analysis method to predict the impact of shape on annual energy use for office buildings, *Energ. Convers. Manage.* 48 (1) (2007) 300–305.
- [8] Y. Chen, S. Wang, X. Yang, Y. Fan, J. Ge, Y. Li, Temporal variation of wall flow and its influences on energy balance of the building wall, *City Built Environ.* 1 (1) (2023) 3.
- [9] S.B. Sadineni, S. Madala, R.F. Boehm, Passive building energy savings: A review of building envelope components, *Renew. Sustain. Energy Rev.* 15 (8) (2011) 3617–3631.
- [10] S.J. Quan, C. Li, Urban form and building energy use: A systematic review of measures, mechanisms, and methodologies, *Renew. Sustain. Energy Rev.* 139 (2021) 110662.
- [11] E. Resch, R.A. Bohne, T. Kvamsdal, J. Lohne, Impact of urban density and building height on energy use in cities, *Energy Procedia* 96 (2016) 800–814.
- [12] O.S. Asfour, E.S. Alshawaf, Effect of housing density on energy efficiency of buildings located in hot climates, *Energ. Buildings* 91 (2015) 131–138.
- [13] C. Yu, W. Pan, Interbuilding effect on building energy consumption in high-density city contexts, *Energ. Buildings* 278 (2023) 112632.
- [14] T. Ichinose, L. Lei, Y. Lin, Impacts of shading effect from nearby buildings on heating and cooling energy consumption in hot summer and cold winter zone of China, *Energ. Buildings* 136 (2017) 199–210.
- [15] P. Lin, Z. Gou, S.S.Y. Lau, H. Qin, The impact of urban design descriptors on outdoor thermal environment: A literature review, *Energies* 10 (12) (2017) 2151.
- [16] H. Li, K. Zhong, J. Yu, Y. Kang, Z.J. Zhai, Solar energy absorption effect of buildings in hot summer and cold winter climate zone, China, *Solar Energy* 198 (2020) 519–528.
- [17] H. Liu, Y. Pan, Y. Yang, Z. Huang, Evaluating the impact of shading from surrounding buildings on heating/cooling energy demands of different community forms, *Build. Environ.* 206 (2021) 108322.
- [18] F. Ascione, N. Bianco, T. Iovane, M. Mastellone, G.M. Mauro, Is it fundamental to model the interbuilding effect for reliable building energy simulations? Interaction with shading systems, *Build. Environ.* 183 (2020) 107161.1.
- [19] Y. Sun, G. Augenbroe, Urban heat island effect on energy application studies of office buildings, *Energ. Buildings* 77 (2014) 171–179.
- [20] Y. Liu, R. Stouffs, A. Tablada, N.H. Wong, J. Zhang, Comparing microscale weather data to building energy consumption in Singapore, *Energ. Buildings* 152 (2017) 776–791.
- [21] E. Erell, T. Williamson, Simulating air temperature in an urban street canyon in all weather conditions using measured data at a reference meteorological station, *Int. J. Climatol.* 26 (12) (2006) 1671–1694.
- [22] P. Agee, L. Nikdel, S. Roberts, A measured energy use, solar production, and building air leakage dataset for a zero-energy commercial building, *Sci. Data* 8 (1) (2021) 299.
- [23] G.B. Mohurd, 50176–2016 Thermal Design Code for Civil Building, China Architecture and Building Press, Beijing, 2016.
- [24] B. Bueno, L. Norford, J. Hidalgo, G. Pigeon, The urban weather generator, *J. Build. Perform. Simul.* 6 (4) (2013) 269–281.
- [25] T. Bentham, R. Britter, Spatially averaged flow within obstacle arrays, *Atmos. Environ.* 37 (15) (2003) 2037–2043.
- [26] J. Mao, J.H. Yang, A. Afshari, L.K. Norford, Global sensitivity analysis of an urban microclimate system under uncertainty: Design and case study, *Build. Environ.* 124 (2017) 153–170.
- [27] K. Hämmerberg, M. Vuckovic, A. Mahdavi, Approaches to urban weather modelling: a Vienna case study, *Appl. Mech. Mater.* 887 (2019) 344–352.
- [28] Agee, Philip, and Leila Nikdel. An Energy Use, Energy Production, and Building Air Leakage Dataset for a Zero Energy Commercial Building. OSF, 6 July 2021. Web.
- [29] G. Mutani, V. Todeschi, Building energy modelling at neighborhood scale, *Energ. Effi.* 13 (7) (2020) 1353–1386.
- [30] Y. Fan, Z. Wang, Y. Li, K. Wang, Z. Sun, J. Ge, Urban heat island reduces annual building energy consumption and temperature related mortality in severe cold region of China, *Urban Clim.* 45 (2022) 101262.
- [31] National Bureau of Statistics of China. National Bureau of Statistics of China. China Statistic Year Book 2012, 2012.
- [32] J. Allegri, V. Dorer, J. Carmeliet, Influence of the urban microclimate in street canyons on the energy demand for space cooling and heating of buildings, *Energ. Buildings* 55 (2012) 823–832.
- [33] L.S. Chan, Investigating the thermal performance and Overall Thermal Transfer Value (OTTV) of air-conditioned buildings under the effect of adjacent shading against solar radiation, *J. Build. Eng.* 44 (2021) 103211.
- [34] J. Park, J.H. Kim, W. Sohn, D.K. Lee, Urban cooling factors: Do small greenspaces outperform building shade in mitigating urban heat island intensity? *Urban For. Urban Green.* 64 (2021) 127256.
- [35] C. Xi, C. Ren, J. Wang, Z. Feng, S.J. Cao, Impacts of urban-scale building height diversity on urban climates: A case study of Nanjing, China, *Energy Build.* 251 (2021) 111350.
- [36] Y. Li, S. Schubert, J.P. Kropp, D. Rybski, On the influence of density and morphology on the Urban Heat Island intensity, *Nat. Commun.* 11 (1) (2020) 2647.
- [37] A.L. Pisello, V.L. Castaldo, J.E. Taylor, F. Cotana, Expanding Inter-Building Effect modelling to examine primary energy for lighting, *Energ. Buildings* 76 (2014) 513–523.
- [38] A.L. Pisello, J.E. Taylor, X. Xu, F. Cotana, Interbuilding effect: Simulating the impact of a network of buildings on the accuracy of building energy performance predictions, *Build. Environ.* 58 (2012) 37–45.
- [39] Y. Han, J.E. Taylor, A.L. Pisello, Toward mitigating urban heat island effects: investigating the thermal-energy impact of bioinspired retro-reflective building envelopes in dense urban settings, *Energy Build.* 102 (2015) 380–389.
- [40] C. Hong, Y. Wang, Z. Gu, How to understand the heat island effects in high-rise compact urban canopy? *City Built Environ.* 1 (1) (2023) 2.
- [41] J.A. Diaz-Acevedo, L.F. Grisales-Noreña, A. Escobar, A method for estimating electricity consumption patterns of buildings to implement Energy Management Systems, *J. Build. Eng.* 25 (2019) 100774.
- [42] D.H.W. Li, S.L. Wong, Daylighting and energy implications due to shading effects from nearby buildings, *Appl. Energy* 84 (12) (2007) 1199–1209.
- [43] A. Dutta, A. Samanta, S. Neogi, Influence of orientation and the impact of external window shading on building thermal performance in tropical climate, *Energ. Buildings* 139 (2017) 680–689.
- [44] Y. Zou, Y. Deng, D. Xia, S. Lou, X. Yang, Y. Huang, Z. Zhong, Comprehensive analysis on the energy resilience performance of urban residential sector in hot-humid area of China under climate change, *Sustain. Cities Soc.* 88 (2023) 104233.
- [45] C. Spandagos, T.L. Ng, Equivalent full-load hours for assessing climate change impact on building cooling and heating energy consumption in large Asian cities, *Appl. Energy* 189 (2017) 352–368.
- [46] L. Biao, J. Cunyan, W. Lu, C. Weihua, L. Jing, A parametric study of the effect of building layout on wind flow over an urban area, *Build. Environ.* 160 (2019) 106160.
- [47] A. Salvati, P. Monti, H.C. Roura, C. Cecere, Climatic performance of urban textures: Analysis tools for a Mediterranean urban context, *Energ. Buildings* 185 (2019) 162–179.
- [48] W. Kuttler, S. Weber, Characteristics and phenomena of the urban climate, *Meteorol. Z.* (2023).
- [49] A. Ahmed, A. Khalid, B. Ahmed, G.S. Mohsin, Impact of solar radiation on building envelope using energyplus software, Karachi, Pakistan, SIMEC, 2017, pp. 24–25.

- [50] Y. Fan, X. Ding, J. Wu, J. Ge, Y. Li, High spatial-resolution classification of urban surfaces using a deep learning method, *Build. Environ.* 200 (2021) 107949.
- [51] X. Ding, Y. Fan, Y. Li, J. Ge, Urban surface classification using semi-supervised domain adaptive deep learning models and its application in urban environment studies, *Environ. Sci. Pollut. Res.* (2023) 1–20.
- [52] A. Boccalatte, M. Fossa, L. Gaillard, et al., Microclimate and urban morphology effects on building energy demand in different European cities, *Energ. Buildings* 224 (2020) 110129.
- [53] S. Song, H. Leng, H. Xu, et al., Impact of urban morphology and climate on heating energy consumption of buildings in severe cold regions, *Int. J. Environ. Res. Public Health* 17 (22) (2020) 8354.
- [54] L.L.H. Peng, Z. Jiang, et al., Impact of urban heat island on energy demand in buildings: Local climate zones in Nanjing, *Appl. Energy* 260 (2020) 114279.
- [55] Y. Liu, Q. Li, L. Yang, et al., Urban heat island effects of various urban morphologies under regional climate conditions, *Sci. Total Environ.* 743 (2020) 140589.
- [56] I.D. Stewart, T.R. Oke, Local climate zones for urban temperature studies, *Bull. Am. Meteorol. Soc.* 93 (12) (2012) 1879–1900.
- [57] J.M. Sobstyl, T. Emig, M.J.A. Qomi, et al., Role of city texture in urban heat islands at nighttime, *Phys. Rev. Lett.* 120 (10) (2018) 108701.
- [58] G. Chen, D. Wang, Q. Wang, et al., Scaled outdoor experimental studies of urban thermal environment in street canyon models with various aspect ratios and thermal storage, *Sci. Total Environ.* 726 (2020) 138147.
- [59] D. Lai, W. Liu, T. Gan, et al., A review of mitigating strategies to improve the thermal environment and thermal comfort in urban outdoor spaces, *Sci. Total Environ.* 661 (2019) 337–353.
- [60] F.B. Errebai, D. Strelbel, J. Carmeliet, et al., Impact of urban heat island on cooling energy demand for residential building in Montreal using meteorological simulations and weather station observations, *Energ. Buildings* 273 (2022) 112410.
- [61] A.L. Pisello, V.L. Castaldo, J.E. Taylor, et al., The impact of natural ventilation on building energy requirement at inter-building scale, *Energ. Buildings* 127 (2016) 870–883.
- [62] K. Javanroodi, M. Mahdavinejad, V.M. Nik, Impacts of urban morphology on reducing cooling load and increasing ventilation potential in hot-arid climate, *Appl. Energy* 231 (2018) 714–746.
- [63] I. Lima, V. Scalco, R. Lamberts, Estimating the impact of urban densification on high-rise office building cooling loads in a hot and humid climate, *Energ. Buildings* 182 (2019) 30–44.
- [64] J. Wen, Y. Xie, S. Yang, et al., Study of surrounding buildings' shading effect on solar radiation through windows in different climates, *Sustain. Cities Soc.* 86 (2022) 104143.
- [65] Y.J. Ahn, D.W. Sohn, The effect of neighbourhood-level urban form on residential building energy use: A GIS-based model using building energy benchmarking data in Seattle, *Energ. Buildings* 196 (2019) 124–133.
- [66] GB 51350-2019, Technical Standard for Nearly-Zero Energy Building, China Architecture & Building Press, Beijing, China, 2019.
- [67] GB 50189-2005, Design standard for energy efficiency of public buildings, China Architecture & Building Press, Beijing, China, 2005.
- [68] N. Lauzet, A. Rodler, M. Musy, et al., How building energy models take the local climate into account in an urban context—A review, *Renew. Sustain. Energy Rev.* 116 (2019) 109390.
- [69] GB 55015-2021; General code for building energy conservation and renewable energy utilization. Housing and Rural Construction, Beijing, China, 2021.
- [70] GB 50189-2015; Standard for energy efficiency design of public buildings. Ministry of Housing and Urban - Rural Development of the People's Republic of China. Beijing, China, 2012.
- [71] G.E. Jian, L.V. Guoquan, T. Jiahuan, Z. Kang, Building decarbonization based on building loads flexibility and clusters' collaboration, *National Science Open* (2024). ISSN 2097–1168.